2014

Acute reduction of microglia does not alter axonal injury in a mouse model of repetitive concussive traumatic brain injury

Rachel E. Bennett
Washington University School of Medicine

David L. Brody
Washington University School of Medicine

JOURNAL OF NEUROTRAUMA 31:1647–1663 (October 1, 2014)

DOI: 10.1089/neu.2013.3320

Acute Reduction of Microglia Does Not Alter Axonal Injury in a Mouse Model of Repetitive Concussive Traumatic Brain Injury

Rachel E. Bennett and David L. Brody

Abstract

The pathological processes that lead to long-term consequences of multiple concussions are unclear. Primary mechanical damage to axons during concussion is likely to contribute to dysfunction. Secondary damage has been hypothesized to be induced or exacerbated by inflammation. The main inflammatory cells in the brain are microglia, a type of macrophage. This research sought to determine the contribution of microglia to axon degeneration after repetitive closed-skull traumatic brain injury (rcTBI) using CD11b-TK (thymidine kinase) mice, a valganciclovir-inducible model of macrophage depletion. Low-dose (1 mg/mL) valganciclovir was found to reduce the microglial population in the corpus callosum and external capsule by 35% after rcTBI in CD11b-TK mice. At both acute (7 days) and subacute (21 days) time points after rcTBI, reduction of the microglial population did not alter the extent of axon injury as visualized by silver staining. Further reduction of the microglial population by 56%, using an intermediate dose (10 mg/mL), also did not alter the extent of silver staining, amyloid precursor protein accumulation, neurofilament labeling, or axon injury evident by electron microscopy at 7 days postinjury. Longer treatment of CD11b-TK mice with intermediate dose and treatment for 14 days with high-dose (50 mg/mL) valganciclovir were both found to be toxic in this injury model. Altogether, these data are most consistent with the idea that microglia do not contribute to acute axon degeneration after multiple concussive injuries. The possibility of longer-term effects on axon structure or function cannot be ruled out. Nonetheless, alternative strategies directly targeting injury to axons may be a more beneficial approach to concussion treatment than targeting secondary processes of microglial-driven inflammation.

Key words: axon injury; concussion; microglia

Introduction

While 91% of athletes will recover from symptoms of concussion within 1 week, there is increasing awareness of the long-term consequences of suffering one or more concussions, particularly among retired professional football players and boxers.[1–9] While the origins of these long-term effects are unknown, studies in postmortem samples from human traumatic brain inury (TBI) and from individuals known to have received multiple concussive injuries have consistently revealed the presence of degenerating axons and inflammation months to years after the initial insult.[10–17] These processes have also been viewed *in vivo* using diffusion tensor imaging to visualize white matter (WM) injury in concussed individuals and using positron emission tomography ligands to the peripheral benzodiazepine receptor to confirm the presence of microglia and macrophage in TBI patients.[18–24] Our group and others have developed mouse models of mild repetitive concussion and have also observed the presence of injured axons within WM and accumulation of glial cells.[25–30] Interestingly, in our repetitive closed-skull injury model, we have observed that accumulation and activation of microglia within WM regions precedes the degeneration of axons as visualized by silver staining.[29] Altogether, these data have led us to hypothesize that microglia and macrophage may contribute to secondary axon injury processes after concussion.

To address this hypothesis we used a CD11b-TK (thymidine kinase) transgenic mouse model to reduce the numbers of microglia within the corpus callosum (CC) and external capsule (EC). CD11b-TK mice express a mutated form of TK from herpes simplex virus (HSV) under the CD11b promoter.[31] When mice are treated with the nucleotide analog, ganciclovir, or its more soluble prolog, valganciclovir, the drug is metabolized by cells expressing TK into a toxic product that leads to cell death. Valganciclovir will only become toxic to $CD11b^+$ cells expressing HSV TK and is not toxic to genetically wild-type (WT) mice, such as the $CD11b\text{-}TK^{-/-}$ littermate controls. Research from other groups has shown that daily intraperitoneal (i.p.) injection of ganciclovir into these mice effectively depletes circulating macrophages and prevents proliferation of microglia in the

Department of Neurology, Washington University, St. Louis, Missouri.

Table 1. Primer Sets Used for qPCR

Encoded protein	*Accession no.*	*Direction*	*5′-3′*	*Amplicon size (bp)*
PGK1	NM_008828.2	Forward Reverse	ctccgctttcatgtagaggaag gacatctcctagtttggacagtg	117
GAPDH	NM_008084	Forward Reverse	catggacttccgtgttccta gcggcacgtcagatcca	55
HPRT1	NM_013556.2	Forward Reverse	cctaagatgagcgcaagttgaa ccacaggactagaacacctgctaa	86
IL1-β	NM_008361.3	Forward Reverse	acggaccccaaaagatgaag ttctccacagccacaatgag	139
IL-6	NM_031168.1	Forward Reverse	caaagccagagtccttcagag gtccttagccactccttctg	150
iNOS	NM_010927	Forward Reverse	tggtccgcaagagagtgct cctcattggccagctgctt	108
CCL2	NM_011333	Forward Reverse	aggtgtcccaaagaagctgta atgtctggacccattccttct	85
TNF-α	NM_013693	Forward Reverse	cttctgtctactgaacttaggg caggcttgtcactcgaattttg	134

qPCR, quantitative polymerase chain reaction; PGK1, phosphoglycerate kinase 1; GAPDH, glyceraldehyde 3-phosphate dehydrogenase; HPRT1, hypoxanthine phosphoribosyltransferase 1; IL, interleukin; iNOS, inducible nitric oxide synthetase; CCL2, chemokine (C-C motif) ligand 2; TNF-α, tumor necrosis factor alpha; bp, base pairs.

brain.[31,32] Here, we show that intracerebroventricular (i.c.v.) delivery of different doses of valganciclovir resulted in a dose-dependent reduction of microglial cells in mice subjected to repetitive closed-skull injury. The effects of reducing the microglial population on both acute and subacute axon degeneration after injury were assessed by silver staining. We found that reducing the number of microglial/macrophage cells had little effect on the amount of axon degeneration at either 7 or 21 days postinjury.

Methods

Animals

CD11b-TK mice were acquired from Jean-Pierre Julien at Laval University (Québec City, Québec, Canada). CD11b-TK mice express HSV TK under the CD11b promoter expressed in microglia and macrophage. Male CD11b-TK$^{+/-}$ founder mice were crossed to C57bl/6j female mice (catalog no.: 000664; JAX; The Jackson Laboratory, Bar Harbor, ME). The resulting offspring were genotyped using previously published methods.[31] Mice carrying the CD11b-TK transgene were termed CD11b-TK$^{+/-}$ mice, and littermates not carrying the transgene were termed CD11b-TK$^{-/-}$ mice and are genetically WT. All mice were housed under a 12-h light/dark cycle and given food and water *ad libitum* in accord with the protocols of the animal studies committee at Washington University (St. Louis, MO).

Osmotic pumps

Alzet osmotic pumps (catalog nos.: 1002 and 2004; DURECT Corporation, Cupertino, CA) with flow rates of 0.25 μL/h were used for these experiments. A complete description of pump assembly can be found elsewhere.[33] Briefly, cannula tubing (catalog no.: 312VT) and osmotic pump connector cannula (catalog no.: 3280PM/SP, cut 2.5 mm below pedestal) were purchased from Plastics One, Inc. (Roanoke, VA). Pump reservoirs were filled with either valganciclovir (catalog no.: SML0191; Sigma-Aldrich, St. Louis, MO) in 0.9% sterile saline (NaCl) or with 0.9% NaCl. Osmotic pump flow tubes were stripped of their plastic caps, and the flow tubes were connected to 1-in lengths of cannula tubing. The other end of the cannula tubing was attached to the osmotic pump connector cannula.

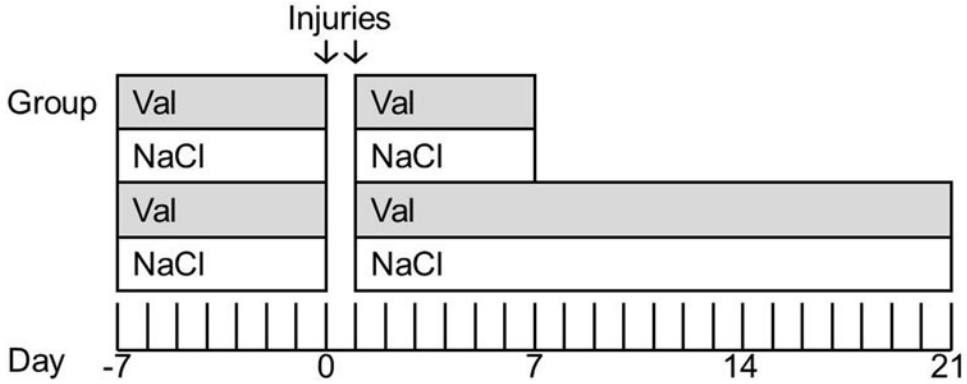

FIG. 1. Experimental design. CD11b-TK$^{+/-}$ or CD11b-TK$^{-/-}$ controls were treated with either valganciclovir or saline by intracerebroventricular osmotic pump for 7 days preceding injury. Pumps were then removed, and a closed-skull or sham injury was performed (day 0). Twenty-four hours later, a second injury was delivered. Pumps were immediately reimplanted, and drug or saline treatment was resumed for another 7 (acute time point) or 21 days (subacute time point). TK, thymidine kinase.

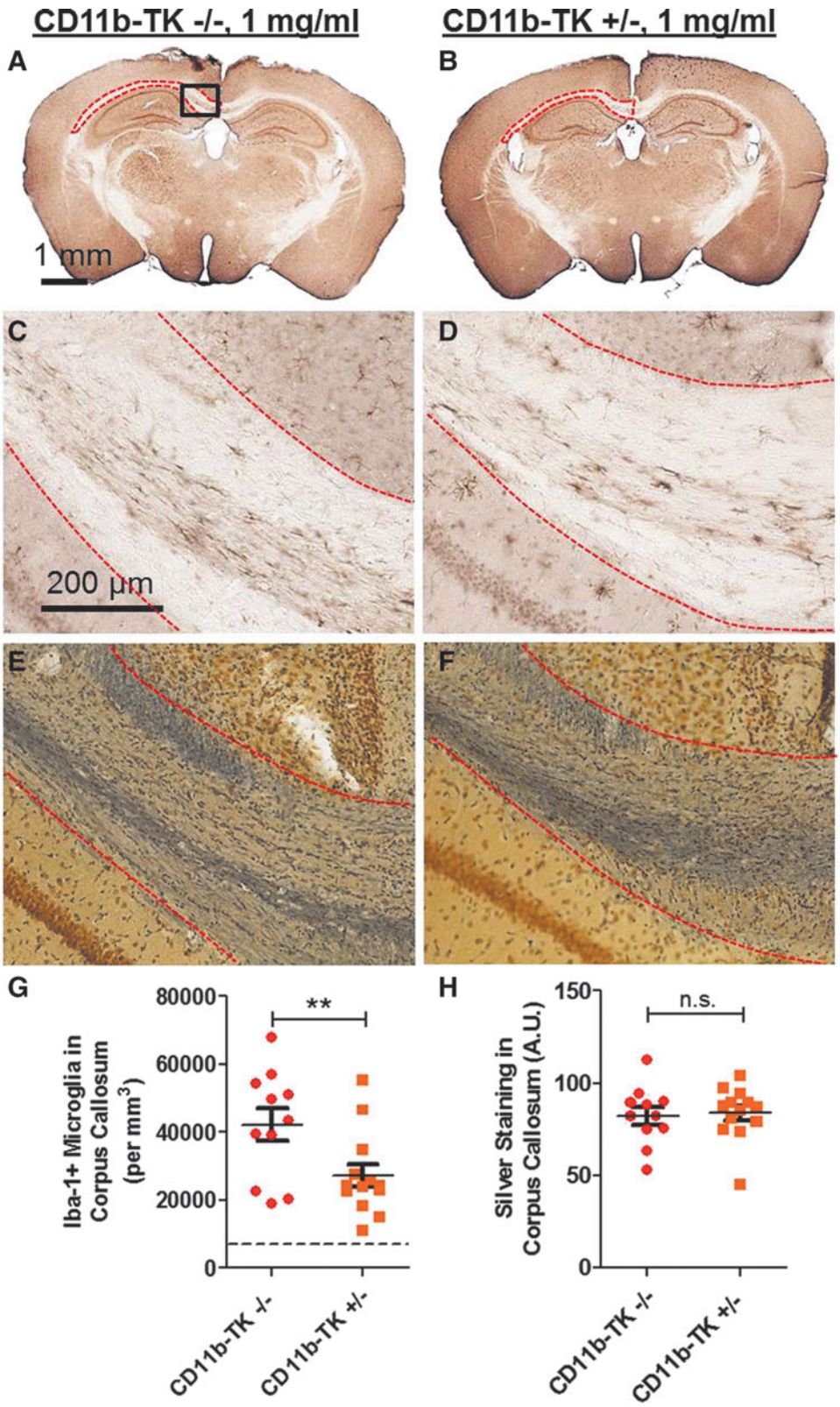

FIG. 2. Treatment of CD11b-TK$^{+/-}$ mice with intracerebroventricular low-dose valganciclovir (1 mg/mL) reduces microglia, but does not affect silver staining 7 days after repetitive closed-skull traumatic brain injury. Iba-1 staining in treated CD11b-TK$^{-/-}$ (**A** and **C**) and CD11b-TK$^{+/-}$ (**B** and **D**) mice. (C and D) Higher magnification views of Iba-1 staining in corpus callosum ipsilateral to injury (region boxed in A, outlined with red dashed line). Silver staining in valganciclovir-treated CD11b-TK$^{-/-}$ (**E**) and CD11b-TK$^{+/-}$ (**F**) mice. (**G**) Stereological quantification of Iba-1-positive microglia in CD11b-TK$^{+/-}$ mice shows a ~35% reduction, compared to controls (one-tailed Student's *t*-test, $^{**}p < 0.01$; dashed line indicates sham levels). (**H**) Silver staining in white matter was unchanged. A.U., arbitrary units; n.s., not significant. Error bars represent standard error of the mean. TK, thymidine kinase. Color image is available online at www.liebertpub.com/neu

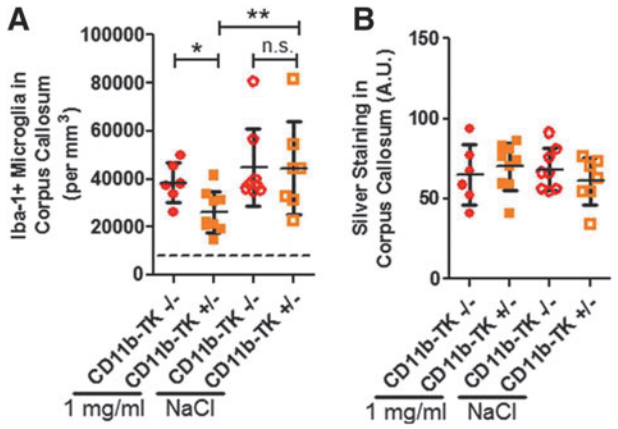

FIG. 3. Low-dose valganciclovir (1 mg/mL), but not saline, reduces microglia and has no effect on silver staining 7 days after injury in an independent cohort of mice. (**A**) Iba-1 staining and (**B**) silver staining in corpus callosum and external capsule of $CD11b^{+/-}$ and $CD11b^{-/-}$ mice receiving either drug or vehicle treatment. A.U., arbitrary units; n.s., not significant. $^{*}p < 0.05$; $^{**}p < 0.01$. Dashed line indicates sham levels. Error bars represent standard error of the mean. TK, thymidine kinase. Color image is available online at www.liebertpub.com/neu

The entire assembly was primed by placing the reservoir in conical tubes containing 0.9% NaCl, and tubes were stored at 37°C for 36–48 h before implantation. This longer priming step was deemed necessary because cannula tubing was not filled with drug—preliminary experiments with 1.5% Evan's blue in saline showed that it takes ~36 h for solution to travel from the reservoir of 14-day 0.25-μL/h pumps to the end of the cannula under these conditions.

Surgical procedures

Six to 8-week-old CD11b-$TK^{+/-}$ and WT littermate controls were used in all experiments. Mice were randomly assigned to either NaCl or valganciclovir treatment groups. For implantation of osmotic pumps, mice received inhaled isofluorane anesthesia and the head was fixed in a stereotaxic frame. Temperature was regulated using a heat pad (Sun Microsystems II; Sun Microsystems, Inc., Santa Clara, CA). A midline incision was made to expose the skull and a small (0.9-mm) burr hole was drilled contralateral to the repetitive closed-skull TBI (rcTBI) impact site at anterior/posterior (A/P) −0.84 mm relative to bregma, mediolateral (ML) + 1.5 mm relative to mid-line at bregma. Pumps were implanted subcutaneously, and a drop of cyanoacrylate glue was applied to the bottom of the plastic portion of the cannula. A cannula guide was used to drive the metal osmotic pump connector cannula through the burr hole into the lateral ventricle (dorsoventricular −2.5 mm) and to hold it firmly in place for 1–2 min while the glue set. The top of the cannula was trimmed, and the incision was sutured closed. Mice received antibacterial ointment and were placed on a heat pad for recovery. Once animals were ambulatory, they were housed individually to prevent cagemates from tampering with pumps.

Seven days after pump implantation, pumps were removed, fitted with new cannulas, placed in individual conical tubes containing 0.9% NaCl and 0.01% sodium azide (NaN_3), and stored at 37°C. Mice then received two repetitive closed-skull injuries 24 h apart, as described previously.[29] Briefly, a rubber tip was fitted on an electromagnetic impact device that was used to impact the skull with the tip centered at A/P −1.8, ML −1.5 bregma to a depth of −3.3 mm. Sham-injured mice underwent the same surgical procedures, but did not receive impacts. Immediately after the second impact, pumps were rinsed in filtered phosphate-buffered saline (PBS) and reimplanted as described above to resume drug delivery.

Histology

Mice were sacrificed by isofluorane overdose and decapitation either 7 or 21 days after the first repetitive closed-skull injury. All mice were perfused with 10 mL of cold 0.03% heparin in PBS. Brains were then removed and placed in 4% paraformaldehyde (PFA) for 24–48 h at 4°C and then in 30% sucrose in PBS for 24–48 h at 4°C. Once equilibrated in sucrose, they were frozen on dry ice and sliced into 50-μm sections on a freezing microtome. Serial sections were collected in cryoprotectant (30% ethylene glycol, 15% sucrose, and 0.03 M of phosphate buffer) and stored at 4°C until use.

Immunohistochemistry (IHC) was performed on sections to visualize rabbit polyclonal anti-Iba-1 (catalog no.: 019-19741; Wako Chemicals USA, Inc., Richmond, VA), chicken polyclonal anti–glial fibrillary acidic protein (GFAP; catalog no.: ab4674; Abcam, Cambridge, MA), rabbit polyclonal anti–beta-amyloid precursor protein (β-APP; catalog no.: 512700; Invitrogen, Carlsbad, CA), or mouse monoclonal RM014 (catalog no.: 34-1000; Novex®; Life Technologies, Carlsbad, CA). For this, sections were washed 3 times for 5 min in Tris-buffered saline (TBS), incubated in 0.03% H_2O_2 for 10 min, washed 3 times for 5 min in TBS, then blocked for 30 min in either 3% normal goat serum (NGS; catalog no.: S-1000; Vector Laboratories, Burlingame, CA) or 3% normal donkey serum (catalog no.: 017-000-121; Jackson ImmunoResearch Laboratories, Inc., West Grove, PA) in 0.25% Triton-X TBS (TBS-X). After blocking, primary antibodies (Abs) were applied at a 1:1000 dilution in blocking solution and incubated overnight at 4°C with gentle shaking. The following day, sections were again washed, incubated 1 h at room temperature (RT) in either biotinylated goat

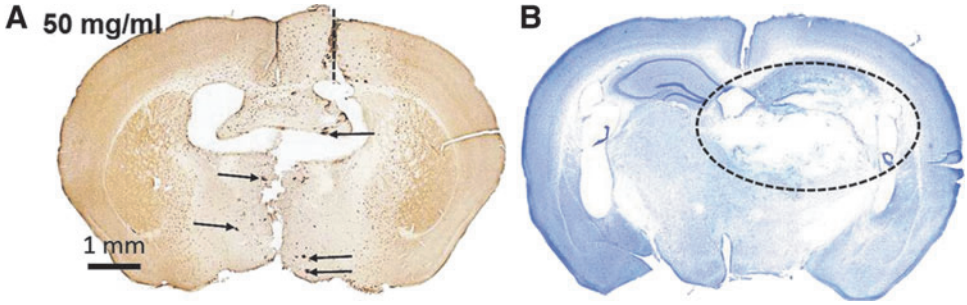

FIG. 4. High-dose (50 mg/mL) valganciclovir treatment was toxic in CD11b-$TK^{+/-}$ mice 7 days postinjury. (**A**) An Iba-1-stained section near the cannula site (dashed line) shows depletion of microglia, but also numerous microhemorrhages (arrows). (**B**) Cresyl violet staining in a section posterior to valganciclovir injection shows extensive tissue loss in the hippocampus and thalamus (dashed oval). TK, thymidine kinase. Color image is available online at www.liebertpub.com/neu

anti-rabbit immunoglobulin G (IgG; catalog no.: BA-1000; Vector Laboratories) or biotinylated donkey anti-chicken IgG (catalog no.: 703-065-155; Jackson ImmunoResearch) secondary Abs were diluted 1:1000 in TBS-X, washed again, then incubated in 1:400 avidin-biotin complex (ABC) reagent (catalog no.: PK-6100; Vector Laboratories) in TBS for another hour. Finally, sections were washed and placed in 3-3′-diaminodebzidine tetrahydrochloride (DAB; catalog no.: D5905) for 5–6 min. After development in DAB, sections were washed, placed on slides, and allowed to air dry, then cover-slipped with cytoseal (catalog no.: 8312-4; Richard-Allan Scientific Co., Kalamazoo, MI). For RM014 staining specifically, the following modifications to the above-described protocol were made: 1) Sections were blocked in 1:10 mouse serum; 2) the primary Ab was incubated 1:2 with biotinylated goat anti-mouse Fab IgG (catalog no.: 115-007-003; Jackson ImmunoResearch) for 20 min before application to the sections overnight; and 3) the secondary Ab was unnecessary, and sections were immediately incubated in ABC on day 2.

Adjacent sets of floating sections were subjected to silver staining (catalog no.: PK301, NeuroSilver Kit II; FD Neurotechnologies, Inc., Elliot City, MD), following the manufacturer's instructions with minor modifications, as previously reported.[29] Sections were incubated for 5 days in PFA before silver staining and were only incubated in solution C once for 2 min.

For cresyl violet staining, sections were rinsed in TBS twice for 5 min, then mounted on glass slides. Once air-dried, they were placed in cresyl violet solution (catalog no.: PS102-1; FD Neurotech) for 5 min, then rinsed and cover-slipped, following manufacturer's protocol.

For terminal deoxynucleotidyl transferase dUTP nick end labeling/neuronal nuclear antigen (TUNEL-NeuN) double-immunofluorescence (IF), 50-μm free-floating sections were washed with TBS and incubated for 15 min with 0.02 mg/mL of proteinase K in TBS. A positive control for TUNEL labeling was generated by incubating a tissue section in 1 μg/mL of DNAse I for 20 min at RT. Sections were then washed and blocked in 3% NGS in TBS-X for 30 min and incubated overnight in 1:1000 rabbit polyclonal anti-NeuN (catalog no.: ABN78; Millipore, Billerica, MA) in blocking solution. The following day, sections were washed and incubated in donkey anti-rabbit IgG cyanine 3 (catalog no.: 711-165-152;

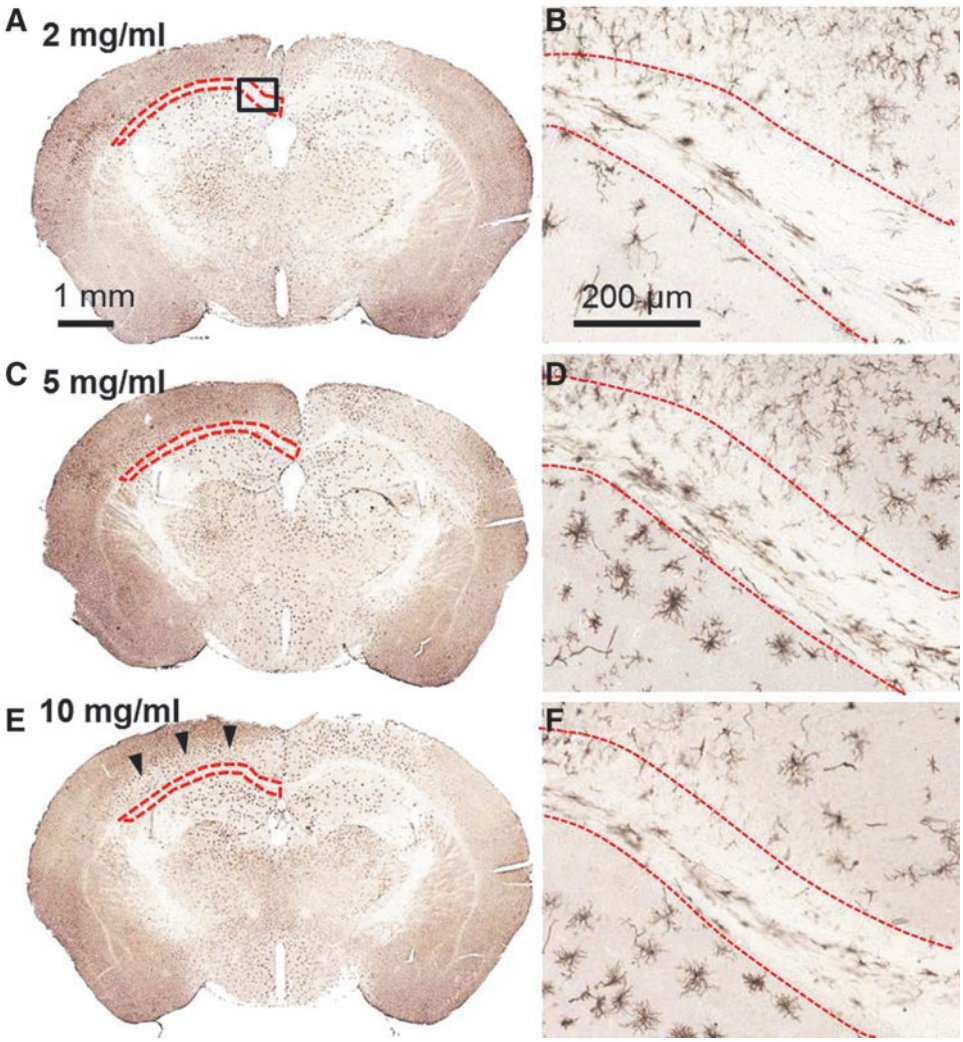

FIG. 5. Valganciclovir dose response in CD11b-TK mice 7 days postinjury. Iba-1-stained whole sections (**A, C,** and **E**) and higher-magnification images (box A) corresponding to the region of interest assessed for iba-1 depletion by stereology (outlined with red dashed line; **B, D,** and **F**). CD11b-TK$^{+/-}$ mice treated with 2 (A and B), 5 (C and D), or 10 mg/mL (E and F) of valganciclovir. Microglial depletion is most prominent ipsilateral to cannulation and drug delivery (right). Arrowheads indicate region of microglial reduction in cortex of hemisphere opposite drug infusion. TK, thymidine kinase. Color image is available online at www.liebertpub.com/neu

Jackson ImmunoResearch) for 1 h at RT in the dark. Sections were then washed, mounted on glass slides, and allowed to air dry for 1 h. A hydrophobic barrier was drawn with a PAP pen around each section, and TUNEL staining was performed according to the FragEL DNA Fragmentation Detection Kit (catalog no.: QIA39; Calbiochem, San Diego, CA), following the manufacturer's instructions. Double IF images were captured using a Zeiss Axiovert 200 laser scanning confocal microscope (Carl Zeiss AG, Oberkochen, Germany).

Electron microscopy

For electron microscopy, mice were perfused with 10 mL of PBS-Heparin followed immediately by 10 mL of 1% PFA, and 1% glutaraldehyde in 0.1 M sodium cacodylate buffer. Brains were fixed using the same solution for 1 h, then sliced into two to three 1-mm coronal slabs per mouse. Slabs were fixed for 5 days before being incubated in 1% osmium tetroxide in sodium cacodylate buffer overnight, followed by dehydration in ascending ethanol series, and

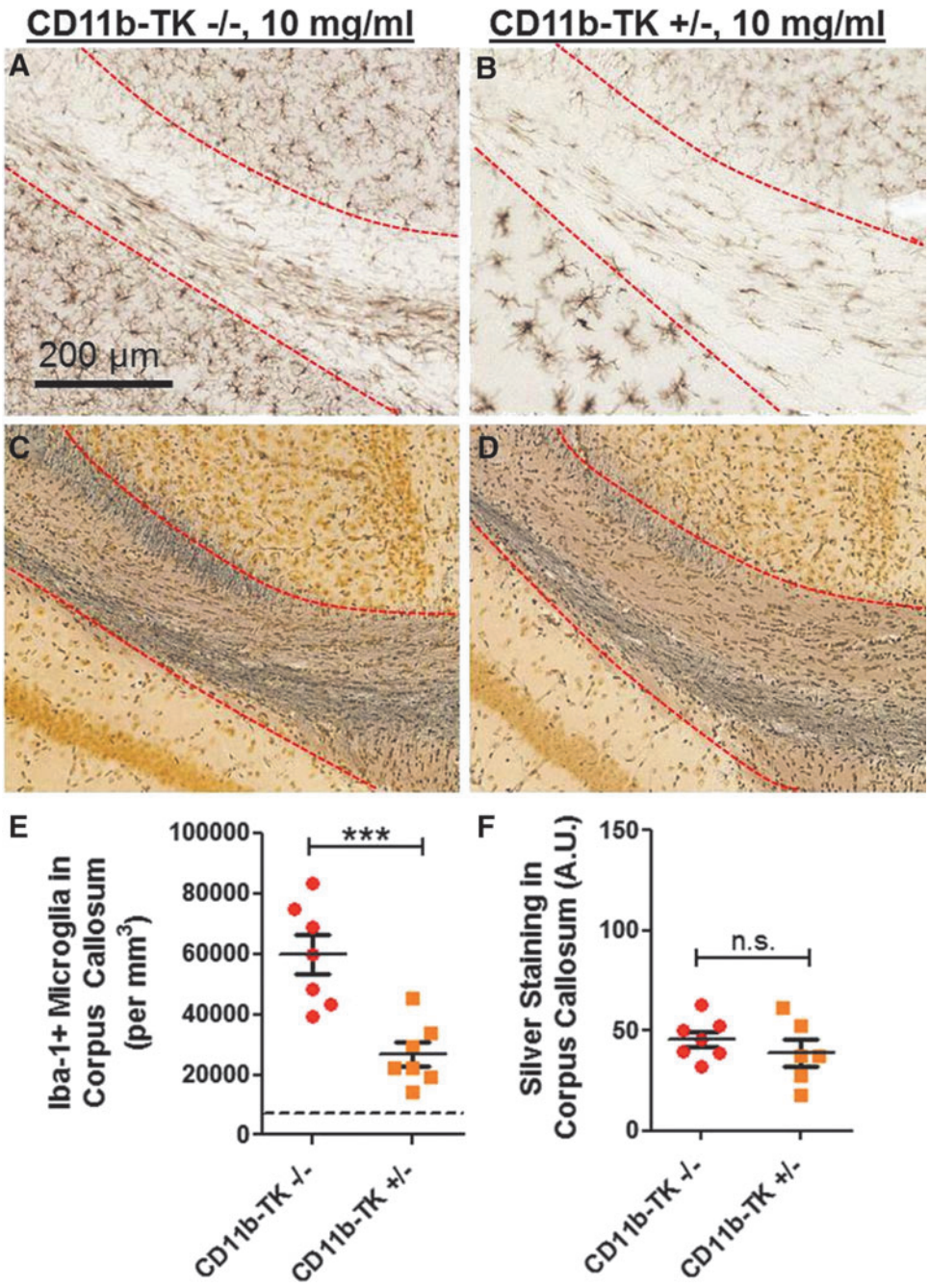

FIG. 6. Acute intermediate-dose valganciclovir (10 mg/mL) reduces Iba-1, but not silver, staining in CD11b-TK mice 7 days after repetitive closed-skull traumatic brain injury. Iba-1 staining in corpus callosum (outlined with red dashed line) in treated CD11b-TK$^{-/-}$ (**A**) and CD11b-TK$^{+/-}$ (**B**) mice. Silver staining in adjacent sections from CD11b-TK$^{-/-}$ (**C**) and CD11b-TK$^{+/-}$ (**D**) mice. (**E**) Iba-1 was reduced by 56% in CD11b-TK$^{+/-}$ mice, compared to controls (one-tailed Student's *t*-test, ***$p < 0.001$; dashed line indicates sham levels). (**F**) No change in silver staining was observed. A.U., arbitrary units; n.s., not significant. Error bars represent standard error of the mean. TK, thymidine kinase. Color image is available online at www.liebertpub.com/neu

embedding Polybed 812 (catalog no.: 08792; Polysciences, Inc., Warrington, PA). Embedding media were cured for 24 h in a dessicator and then in a 60°C oven for 48 h. Semithin sections stained with toluidine blue were prepared using glass knives to identify the region of CC and EC ipsilateral to injury in each coronal slab. Tissue was then thin sectioned (70–90 nm) on a Leica Ultracut E Microtome (Leica Microsystems GmbH, Wetzlar, Germany), stained with 4% uranyl acetate and Reynolds lead citrate, and viewed on a JEOL 100C Electron Microscope (JEOL, Tokyo, Japan). Three to five grids were prepared from each block of tissue, and two blocks (1-mm separation) were prepared from each animal. At least one grid from each block was qualitatively assessed blinded to injury status or genotype for evidence of axonal injury.

Stereological quantification and optical density measurements

For all histological analysis, the region of interest (ROI) was defined to include the CC and EC underlying the impact site. For each mouse, the ROI began with the most anterior section containing hippocampal dentate gyrus (DG) and ended with the most posterior section containing CC fibers that cross mid-line. This yielded 3–4 sections for analysis per animal. The mid-line served as the medial boundary for the ROI, whereas the lateral boundary was formed by drawing a horizontal line between the ventral hippocampus and dorsal thalamus in each coronal section.

Iba-1 stereological methods have been previously published.[29] In brief, stereological quantification was performed blinded to genotype or drug treatment status using StereoInvestigator's (MicroBrightfield) optical fractionator technique. The ROI was traced in each section, and a 180×180 μm grid size and 80×80 μm counting frame was applied to determine the number of Iba-1-positive cells in the CC and EC. This ensured that Gunderson's coefficient of error was < 0.1.

For quantification of silver staining, 20x images were captured of all sections using the Olympus NanoZoomer Whole Slide Imaging System (Olympus Corporation, Tokyo, Japan), as previously reported.[29] From the NanoZoomer file, $1.25\times$ .tiff images of sections containing the DG of the hippocampus and CC were exported and opened in ImageJ software (National Institutes of Health, Bethesda, MD). Background (gold color) was subtracted from each image using the color splitter and image calculator functions, so that only the gray-black silver deposits were visible. ROIs were traced as described for Iba-1 analysis on 32-bit images and measurements were taken to acquire mean gray values corresponding to the intensity of silver staining (0–255) within each ROI. Three serial sections were averaged from each animal to produce a final silver staining value. Optical density measurements were also taken blinded to genotype and drug treatment status.

For GFAP optical density measurements, 5x images of the CC and EC were captured using the NanoZoomer. The .tiff files were converted to 32-bit images in ImageJ, and positive signal on each image was selected using Li's minimum cross-entropy thresholding method, a function of the Auto Threshold plugin. ROIs were selected and drawn as described for Iba-1 stereology and silver staining. The summarize function under analyze particles was used to acquire the area fraction occupied by positive GFAP signal. These values were averaged from three serial sections, and the resulting value is reported.

Quantitative polymerase chain reaction

Quantitative polymerase chain reaction (qPCR) was performed to determine gene expression levels of interleukin (IL)-1β, IL-6, inducible nitric oxide synthetase (iNOS), chemokine (C-C motif) ligand 2 (CCL2), and tumor necrosis factor alpha (TNF-α). Immediately after sacrifice, brains were harvested and a 2-mm coronal slice was collected. The anteriormost portion of the slice

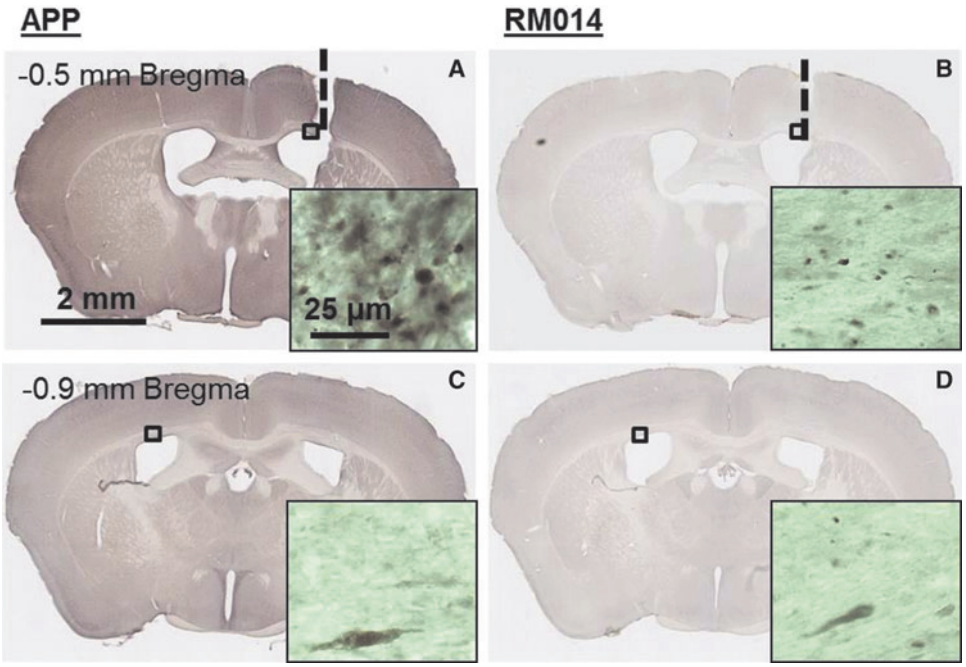

FIG. 7. Amyloid precursor protein (APP) and neurofilament (RM014) labeling in an injured CD11b-TK$^{-/-}$ mouse treated with 10 mg/mL of valganciclovir and sacrificed 7 days postinjury. APP and labeling was prominent at the site of cannulation (dashed line) -0.5 mm relative to bregma (**A** and **B**). Only sparse axonal swellings were detectable in the contralateral hemisphere (injured side) in the corpus callosum and external capsule corresponding to the region of interest assessed for axonal injury in these experiments (**C** and **D**). Insets show higher magnification of labeling in boxed regions in (A) and (C). TK, thymidine kinase. Color image is available online at www.liebertpub.com/neu

corresponded to the anterior end of the hippocampus. The section was further dissected by making a cut parallel to the interface between the hippocampus and thalamus, and only the dorsal portion (approximately 30 mg) was reserved for qPCR. Sections were frozen on crushed dry ice and stored at −80°C. Tissue was later lysed in Qiazol (Qiagen, Jena, Germany) and disrupted using a rotor-stator homogenizer, following the manufacturer's protocol for homogenization of fatty tissues. The final RNA pellet was resuspended in 100 μL of RNAse-free water and further purified using an RNeasy Kit (Qiagen). DNAse was applied to the column to remove genomic DNA contamination. For complementary DNA (cDNA) preparation, 1 μg of RNA was used in each RNA-cDNA reaction (High Capacity RNA-to-cDNA Kit; Applied Biosystems, Foster City, CA). For each qPCR reaction, 1 μL of undiluted cDNA was added to 15 μL of Syber Green PCR Master Mix (Applied Biosystems), 13 uL of ddH_20, and 1 μL of 10-mM forward and reverse primers (Table 1). Samples were loaded on a MicroAmp Fast Optical 96-Well Reaction Plate (Applied Biosystems), and qPCR was carried out on a 7500 Fast Real-Time PCR System (Applied Biosystems). The following conditions were used: 95°C for 10 min followed by 40 cycles of 95°C for 15 sec and 60°C for 1 min.

ΔΔCt values were calculated by normalizing the expression of each gene to the geometric mean of three reference genes (*hprt*, *pgk1*, and *gapdh*). Subsequently, these target gene values were normalized to the arithmentic mean values in untreated naïve mice ($n=4$). Exponential transform was performed to achieve fold-change measures of each gene, where 1 is equal to naïve mice.

Data analysis and statistics

All data were analyzed and graphed using GraphPad Prism software (GraphPad Software Inc., San Diego, CA). Shapiro-Wilks' normality tests were applied to determine whether data were normally distributed. Rank transformations were applied to data that failed

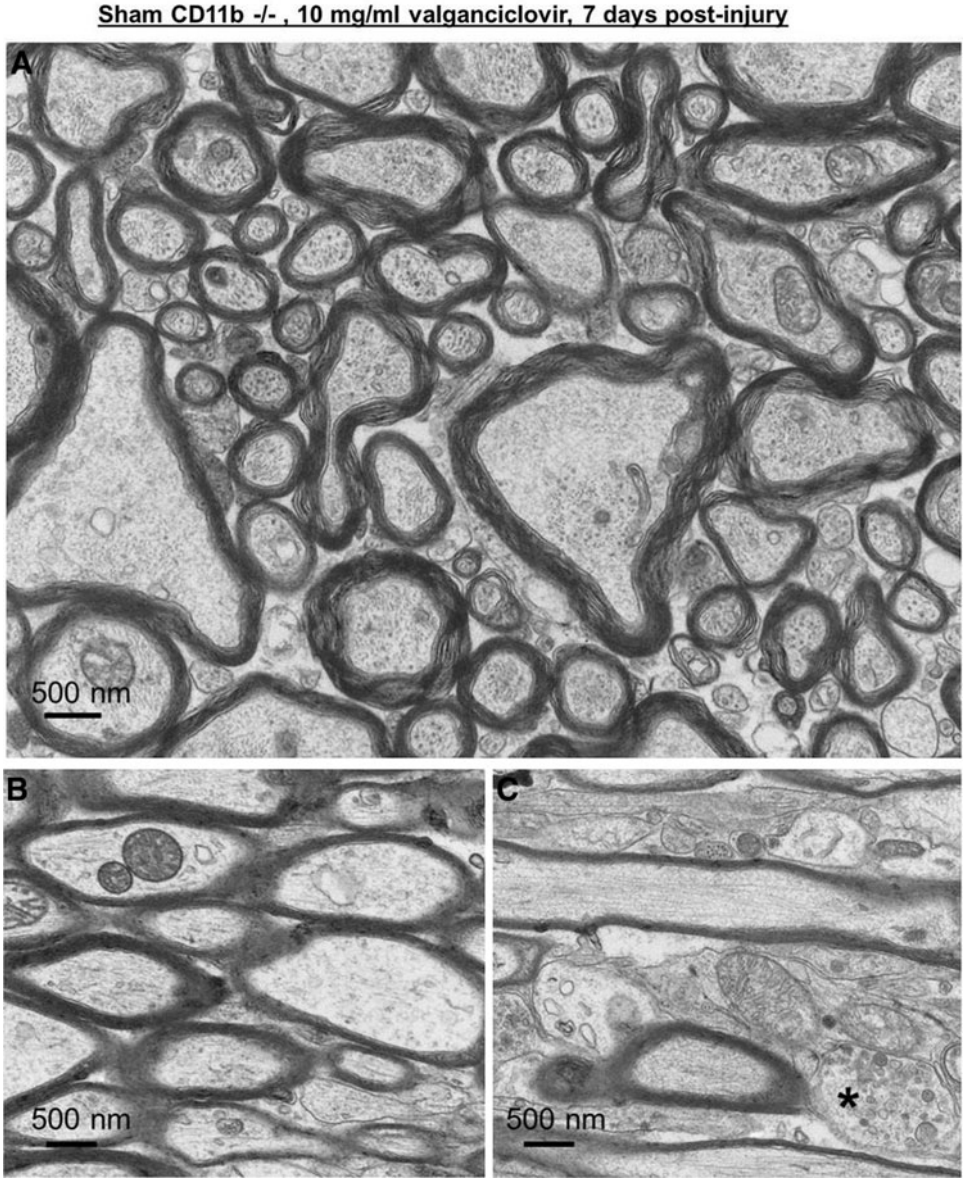

FIG. 8. Normal axonal ultrastructure in a cannulated sham CD11b-$TK^{-/-}$ mouse treated with 10 mg/mL of valganciclovir and sacrificed 7 days post–sham injury. (**A** and **B**) Axons in the corpus callosum near the cingulum display organized cytoskeletal elements and intact myelin sheaths. (**C**) Region containing axons cut parallel to the predominant direction of the corpus callosum. Asterisk (*) indicates a swollen unmyelinated axon with abnormal organelle accumulation. Note nearby axons appear relatively intact, however. TK, thymidine kinase.

normality tests. In experiments with two test groups, Student's *t*-tests were used. Two-way analyses of variance (ANOVAs) were used in all other cases except analysis of sham mice with or without cannulation, in which case a one-way ANOVA was performed. Post-hoc comparisons between CD11b-TK$^{+/-}$ and CD11b-TK$^{-/-}$ mice as well as between saline- and valganciclovir-treated CD11b-TK$^{+/-}$ mice were prespecified. Statistical significance was defined as $p < 0.05$ for *t*-tests and ANOVAs and $p < 0.0167$ for post-hoc tests.

Results

Acute effects of microglia on axonal injury in mice receiving low-dose valganciclovir (7 days)

Previous reports indicate that daily systemic administration of valganciclovir causes hematopoetic toxicity and is fatal to CD11b-TK$^{+/-}$ mice within 10 days.[31] On the other hand, delivery of the drug directly into the brain can result in microglial reduction without the toxicity observed after i.p. injection.[34] Continuous administration is required because macrophages will rapidly repopulate areas of microglial depletion in the absence of the drug.[35] Because our goal was to test the effects of microglial depletion on axonal injury at time points between 1 week and 1 month after injury, we chose to administer valganciclovir continuously by i.c.v. osmotic pump. However, because there is deformation of the brain during the brain injury, we chose to remove the pumps during the 24 h required for the rcTBI procedure to prevent additional injury of the brain caused by the cannula (Fig. 1). For initial experiments, a valganciclovir concentration of 1 mg/mL was chosen because it has been shown by other groups to be effective in reducing microglial cells.[34,36]

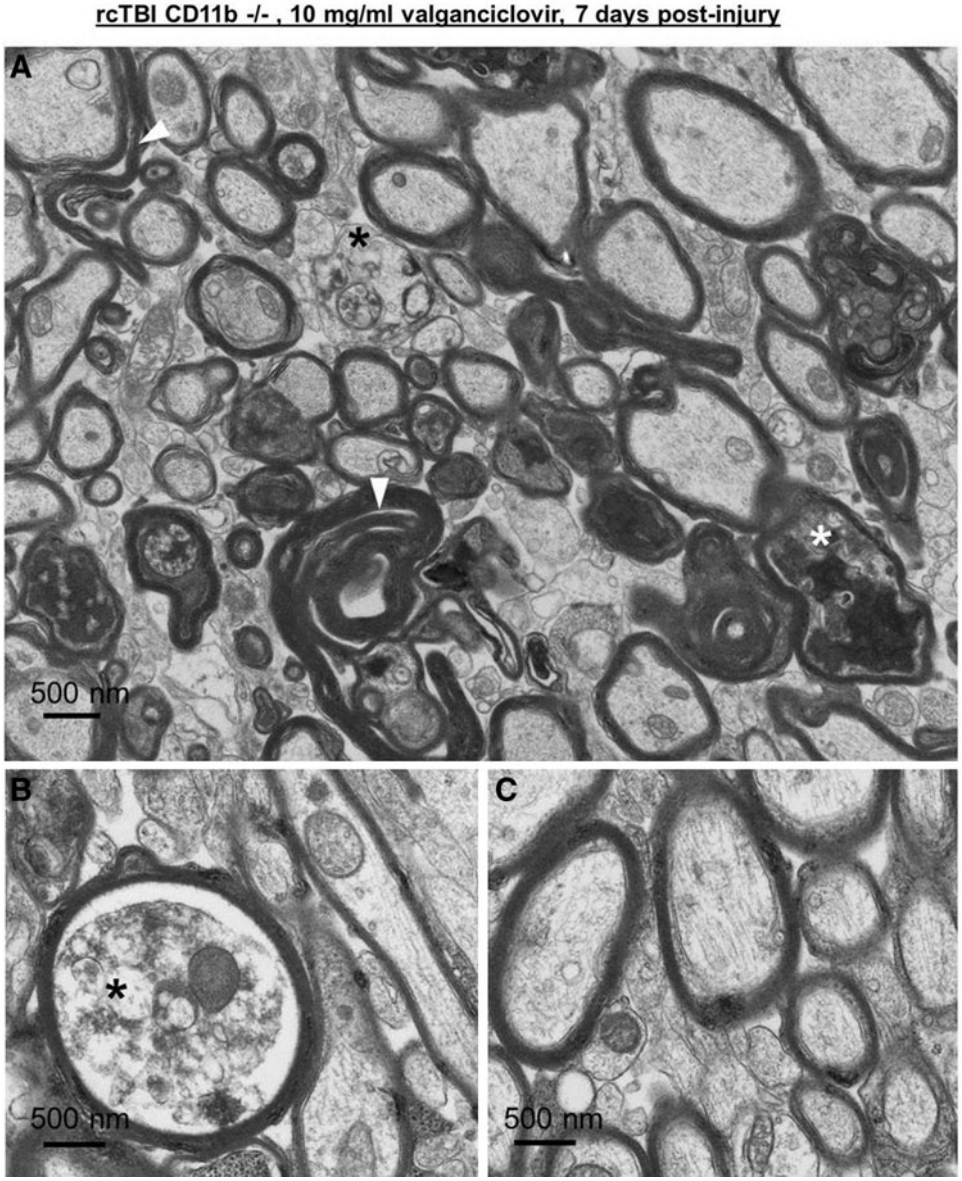

FIG. 9. Ultrastructural abnormalities in an injured CD11b-TK$^{-/-}$ littermate control mouse treated with 10 mg/mL of valganciclovir and sacrificed 7 days postinjury. (**A**) Arrowheads indicate regions of end-stage axonal degeneration in corpus callosum near the cingulum where the axolemma has completely collapsed. Asterisks (*) denote examples of myelinated and unmyelinated axons with organelle accumulation. (**B**) Myelinated axon undergoing Wallerian degeneration (asterisk). (**C**) Region of relatively healthy appearing axons in corpus callosum. rcTBI, repetitive closed-skull traumatic brain injury; TK, thymidine kinase.

Within the ipsilateral CC and EC, treated CD11b-TK$^{+/-}$ mice ($n=13$) had a 35% reduction in the number of microglial cells, compared to littermate controls ($n=11$) at the 7-day time point after injury (one-tailed Student's *t*-test, $p=0.008$; Fig. 2 A–D,G). To control for the effects of injection of vehicle alone, the experiment was repeated with additional groups that received 0.9% NaCl (Fig. 3A; CD11b$^{+/-}$ valganciclovir $n=9$, NaCl $n=7$; CD11b-TK$^{-/-}$ valganciclovir $n=6$, NaCl $n=8$). An effect of genotype ($p=0.0359$) and treatment ($p=0.0226$) was noted, but not an effect of genotype × treatment (two-way ANOVA, $p=0.1039$; Fig. 3A). Prespecified, planned comparisons revealed a significant difference between valganciclovir-treated CD11b-TK$^{+/-}$ versus littermate controls ($p=0.0110$; Fig. 3A), no difference between the two genotypes receiving vehicle alone ($p=0.7096$), and a significant difference between CD11b-TK$^{+/-}$ valganciclovir- and vehicle-treated mice ($p=0.0057$).

We then used silver staining to assess injured axons in mice with reduced numbers of microglia. No difference in the intensity or distribution of silver staining was observed in either the first (two-tailed Student's t-test, $p=0.8292$; Fig. 2E,F,H) or the second groups of mice (two-way ANOVA, genotype $p=0.8478$, treatment $p=0.6147$, genotype × treatment $p=0.2769$; Fig. 3B). We have previously shown that silver staining is a sensitive method to assess axonal injury in this repetitive concussive injury model.[29]

Dose-response of microglia to valganciclovir treatment in CD11b-TK mice

We reasoned that a modest reduction in the number of microglial cells within the WM may not be adequate to produce an effect on the extent of axonal injury. We therefore next tested higher doses of

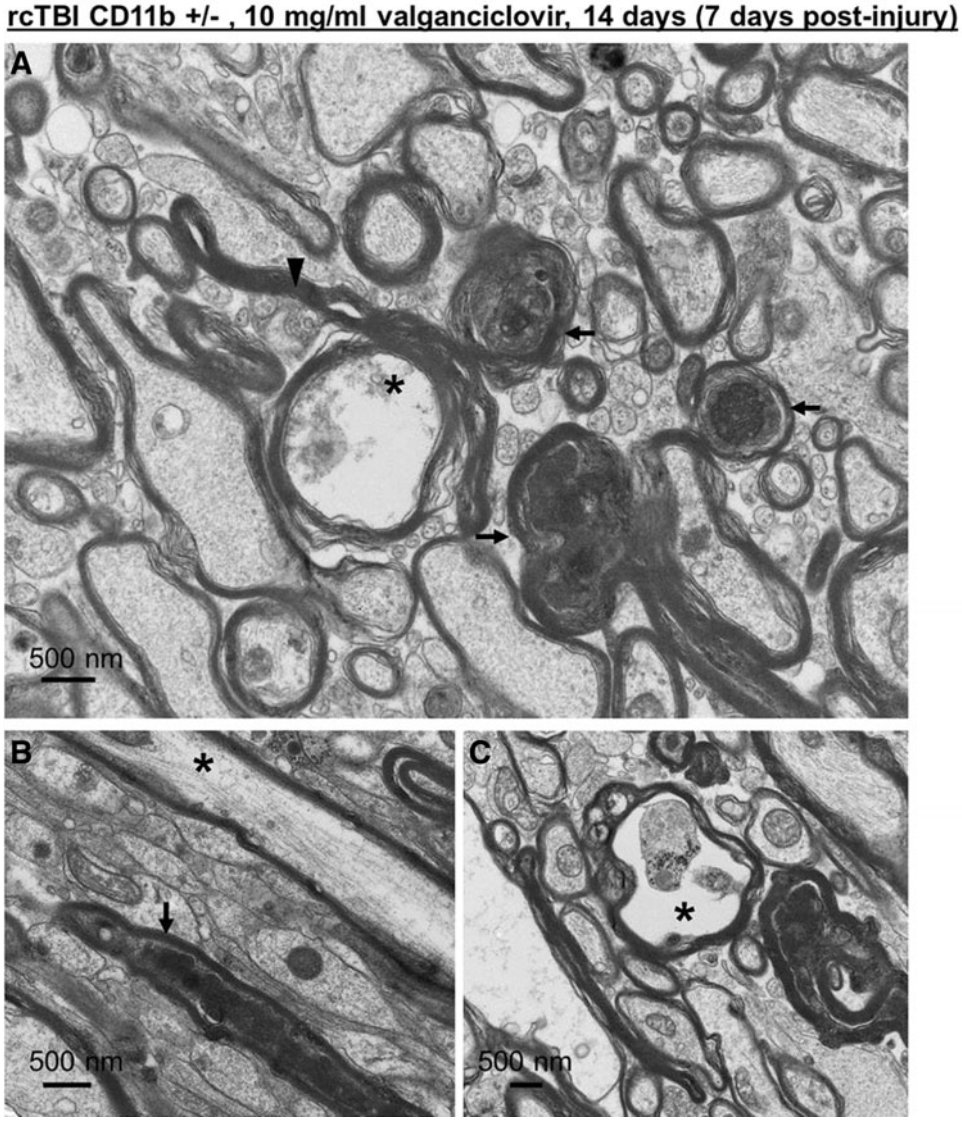

FIG. 10. Ultrastructural abnormalities in an injured CD11b-TK$^{+/-}$ mouse treated with 10 mg/mL of valganciclovir and sacrificed 7 days postinjury. (**A**) Arrowhead indicates an example of end-stage axon degeneration in corpus callosum near the cingulum where the axolemma has completely collapsed. Asterisk (*) denotes a swollen axon undergoing late-stage degeneration, and arrows indicate examples of axons containing densely packed intracellular aggregates. (**B**) Arrow indicates an axon cut parallel to the predominant direction of the corpus callosum with abnormal accumulation of electron-dense intra-axoplasmic material in a region of relatively normal axons (asterisk). (**C**) Asterisk indicates an axon undergoing axolemma collapse. rcTBI, repetitive closed-skull traumatic brain injury; TK, thymidine kinase.

valganciclovir in mice that received rcTBI to increase the amount of microglial depletion. Using the same injection paradigm as before, mice were treated with either 2 ($n=3$), 5 ($n=3$), 10 ($n=5$), or 50 mg/mL ($n=8$) of valganciclovir (Figs. 4 and 5). At 5–7 days postinjury (14 days after initial pump implantation), CD11b-TK$^{+/-}$ mice in the 50-mg/mL group became lethargic, had difficulty walking, and a 50% mortality rate. WT littermate controls treated identically with 50 mg/mL of valganciclovir ($n=6$) appeared normal. Upon histological examination, intraparenchymal hemmorhages and extensive tissue loss within the hippocampus and thalamus were apparent in treated CD11b-TK$^{+/-}$ mice (Fig. 4A,B). Mice that received intermediate doses of 2, 5, or 10 mg/mL appeared normal physically and histologically (Fig. 5A–F). Therefore, 10 mg/mL was selected for future experiments because this dose consistently resulted in microglial depletion in the hemisphere opposite injection near the CC and EC (Fig. 5E,F).

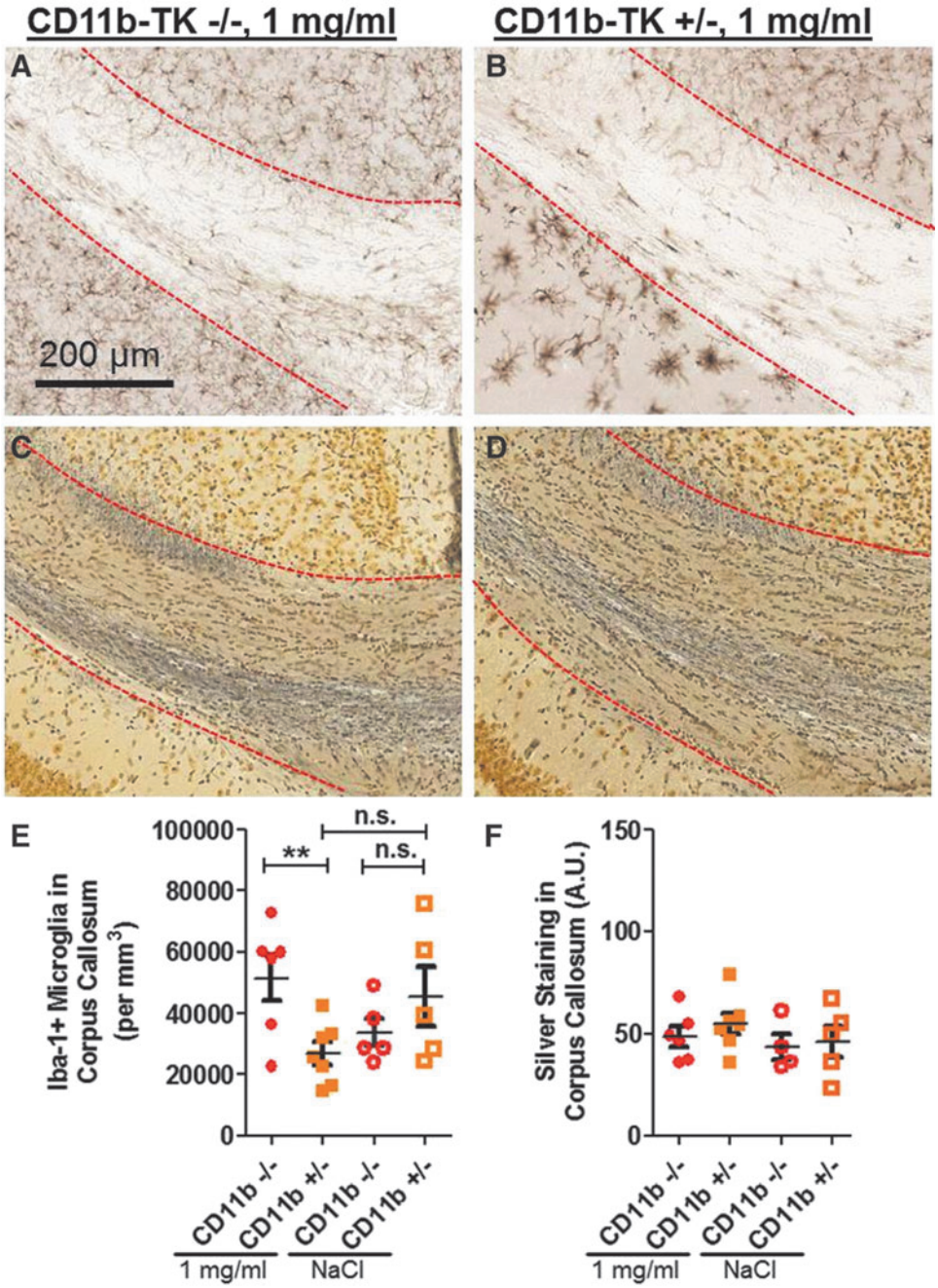

FIG. 11. Treatment with low-dose valganciclovir (1 mg/mL), but not saline, reduces Iba-1, but not silver staining in corpus callosum 21 days after repetitive closed-skull traumatic brain injury. Iba-1 staining in valganciclovir-treated CD11b-TK$^{-/-}$ (**A**) and CD11b-TK$^{+/-}$ (**B**) mice. Silver staining in valganciclovir-treated CD11b-TK$^{-/-}$ (**C**) and CD11b-TK$^{+/-}$ (**D**) mice. (**E**) Iba-1 was reduced by 35% in CD11b-TK$^{+/-}$ mice, compared to CD11b-TK–/– controls (one-tailed Student's *t*-test; $^{**}p<0.01$). (**F**) No change in silver staining was observed. A.U., arbitrary units; n.s., not significant. Error bars represent standard error of the mean. TK, thymidine kinase. Color image is available online at www.liebertpub.com/neu

Acute effects of intermediate-dose valganciclovir on axonal injury (7 days)

A separate cohort of mice was treated with 10 mg/mL of valganciclovir and examined 7 days after rcTBI (Fig. 6A–F). At 7 days postinjury, the number of Iba-1-positive cells within the CC and EC ipsilateral to injury was 56% reduced in CD11b-TK$^{+/-}$ ($n=7$), compared to littermate controls ($n=7$; one-tailed Student's t-test, $p=0.0004$; Fig. 6A,B,E). Again, no significant reduction in the amount of silver staining was observed (two-tailed Student's t-test, $p=0.6045$; Fig. 6C,D,F).

To determine whether other aspects of axonal injury were affected by microglial depletion, other injury markers were assayed in adjacent tissue sections for APP and neurofilament compaction (Fig. 7A–D). APP is a marker of fast axonal transport that accumulates in axonal swellings within hours of axonal injury.[37,38] The neurofilament Ab, RM014, has been used to detect neurofilament compaction, an indicator of cytoskeletal disruption in degenerating axons.[39] Both of these markers were present near the site of cannulation in all mice (Fig. 7A,B), but were sparse and detected infrequently in more-posterior regions ipsilateral to injury (Fig. 7C,D). Most commonly, they occurred in WM tracts overlying the lateral ventricle, which may be a particularly vulnerable region in this model. However, no qualitative difference was observed between genotypes, indicating that these markers of axonal injury were not affected by microglial depletion.

To further confirm that no subtle alterations in axonal injury severity are occurring after microglial depletion, qualitative electron microscopy was carried out in a sham littermate control treated with 10 mg/mL of valganciclovir ($n=1$; Fig. 8 A–C), injured littermate controls treated with 10 mg/mL of valganciclovir ($n=2$; Fig. 9A–C), or CD11b-TK$^{+/-}$ mice treated with 10 mg/mL of valganciclovir ($n=2$; Fig. 10A–C). The frequency and characteristics of axonal injury 7 days postinjury were assessed. The CC and EC ipsilateral to injury directly beneath the impact site were analyzed. In sham injury with 10 mg/mL of valganciclovir treatment, most axons displayed a normal appearance, with intact myelin sheaths and regularly spaced microtubules and neurofilaments (Fig. 8A,B). However, occasional swollen axons displayed organelle accumulation consistent with injury and were likely artifacts of cannulation (Fig. 8C). In contrast, the effects of repetitive concussive TBI were more dramatic. In both CD11b-TK$^{+/-}$ and CD11b-TK$^{-/-}$ mice injured and treated with valganciclovir, axonal injury was a prominent feature within the CC and EC. Notably, small myelinated axons displayed abnormal morphology with organelle accumulation, cytoskeletal disorganization, and axolemma collapse (Figs. 9 and 10). These features are all consistent with Wallerian degeneration. Overall, injury levels were approximately the same as reported previously in this model.[29] No overt differences were detected between CD11b-TK$^{+/-}$ and CD11b-TK$^{-/-}$ mice. These observations were confirmed by a second, blinded observer (Dr. Krikor Dikranian). These observations further indicate that axonal injury was not affected by microglial depletion.

Subacute effects of low- and intermediate-dose valganciclovir on axonal injury (21 days)

Next, we sought to determine whether longer-term reduction of microglia alters the evolution of axonal injury over time (Figs. 11 and 12). We have previously reported that silver staining abnormalities persist out to 49 days (the longest time point analyzed).[29] We chose to analyze mice at 21 days postinjury because this would allow us to treat mice with valganciclovir for 1 month (28 days) and would not require that the osmotic pumps to be replaced—a procedure requiring additional surgery. In the low-dose experiment, mice were treated with 1 mg/mL of valganciclovir (CD11b$^{+/-}$ $n=7$, CD11b$^{-/-}$ $n=6$) or 0.9% NaCl (CD11b$^{+/-}$ $n=5$, CD11b$^{-/-}$ $n=5$; Fig. 11). Overall, analysis of microglial activation by two-way

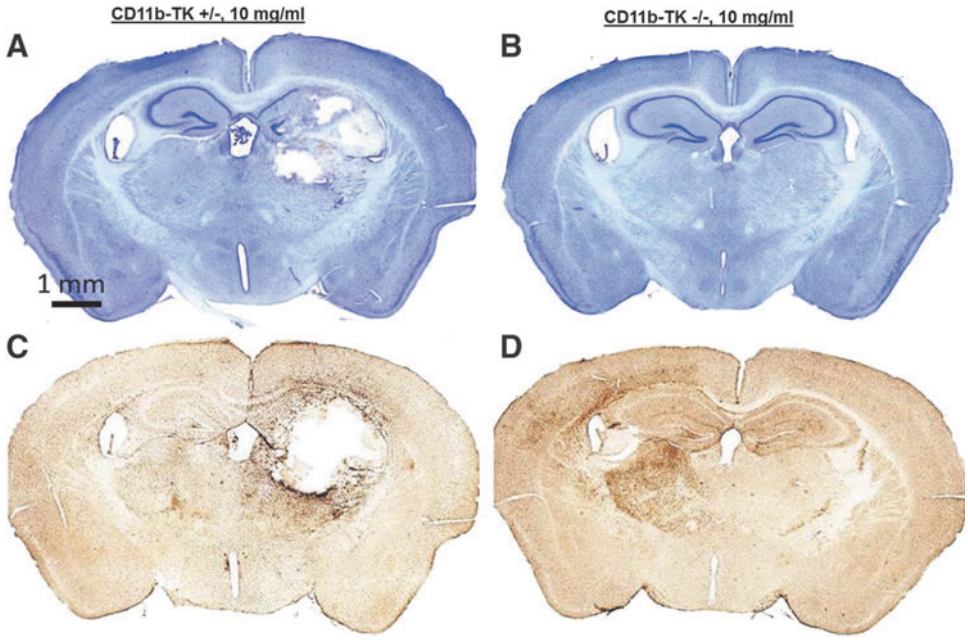

FIG. 12. Subacute treatment with intermediate-dose valganciclovir is toxic in injured CD11b-TK mice. Twenty-eight days total treatment resulted in tissue loss, as visualized by cresyl violet, in hippocampus and thalamus of injured CD11b-TK$^{+/-}$ (**A**), but not CD11b-TK$^{-/-}$ (**B**), mice. Iba-1 staining shows extent of microglial depletion in CD11b-TK$^{+/-}$ (**C**) and not in a CD11b-TK$^{-/-}$ (D) littermate control mouse subjected to repetitive closed-skull traumatic brain injury. TK, thymidine kinase. Color image is available online at www.liebertpub.com/neu

ANOVA revealed no effect of genotype ($p=0.3307$) or treatment ($p=0.9511$), but a significant genotype × treatment interaction ($p=0.0118$). Additionally, a significant reduction of microglial cells in the CC and EC of approximately 35% in valganciclovir-treated CD11b-TK$^{+/-}$ mice, compared to valganciclovir-treated littermate controls, was observed ($p=0.0099$; Fig. 11A,B,E). No difference was observed in NaCl-treated mice between genotypes ($p=0.2488$). The difference between microglial cells in valganciclovir-treated versus NaCl-treated CD11b-TK$^{+/-}$ mice was not quite statistically significant ($p=0.0547$; Fig. 11E). Again, as in the acute experiments, no difference was observed across groups in the amount of silver staining (Fig. 11C,D,F).

An additional group of either CD11b-TK$^{+/-}$ mice ($n=6$) or littermate controls ($n=8$) received 10 mg/mL of valganciclovir and was sacrificed 21 days postinjury (Fig. 12A–D). Though the mice did not display an overtly abnormal behavioral phenotype, histological examination revealed tissue loss similar to that observed with the 50-mg/mL dose. Thus, the duration of drug administration at intermediate doses can also produce a toxic effect in CD11b-TK mice. Because of the clear toxicity of the drug, Iba-1 and silver staining were not quantified in these animals.

Terminal deoxynucleotidyl transferase dUTP nick end labeling labeling in mice treated with intermediate-dose valganciclovir

Given the apparent toxicity of intermediate-dose valganciclovir (10 mg/mL) in CD11b-TK mice treated for 21 days postinjury, we performed TUNEL labeling to determine whether this intermediate dose induces apoptosis in neurons 7 days postinjury (Fig. 13A,B). Sections from CD11b-TK$^{+/-}$ ($n=7$) and CD11b-TK$^{-/-}$ ($n=7$) mice treated with valganciclovir were double labeled for TUNEL and NeuN, a neuron-specific marker. The hippocampal CA3 ipsilateral to cannulation and drug infusion was the focus of these investigations because this is a region significantly affected by toxicity 21 days postinjury. However, no apoptotic neurons were detected here at 7 days postinjury. This would indicate that neurodegeneration begins later than day 7 postinjury. As a positive control to assess the sensitivity of our TUNEL labeling, we treated adjacent sections with DNAse I to induce DNA nicks. This caused prominent TUNEL staining (Fig. 13C). Thus, the lack of TUNEL staining in the valganciclovir-treated CD11b-TK$^{+/-}$ mice is likely to accurately indicate a lack of apoptotic injury.

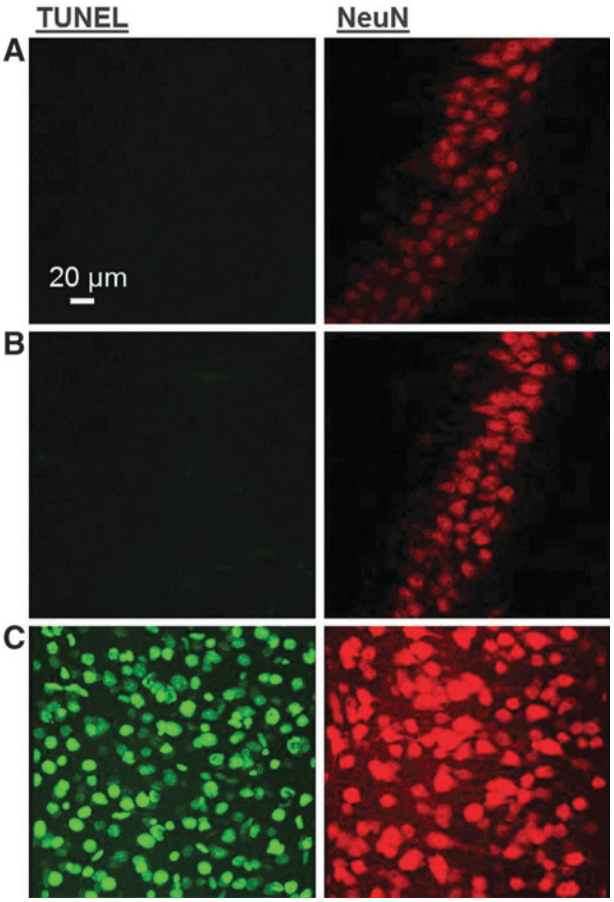

FIG. 13. Double immunofluorescence for TUNEL (green) and NeuN (red) in the hippocampal CA3 does not indicate neuronal apoptosis in injured mice treated with 10 mg/mL of valganciclovir and sacrificed 7 days postinjury. TUNEL labeling was not observed in NeuN^{+} cells in the hippocampal CA3 of CD11b$^{-/-}$ (**A**) or CD11b$^{+/-}$ (**B**) mice. A positive control for TUNEL labeling was generated by incubating a more anterior section (cortical region) in DNAse I to induce double-stranded DNA breaks (**C**). All images were acquired using the same settings on a laser scanning confocal microscope. TUNEL, terminal deoxynucleotidyl transferase dUTP nick end labeling; NeuN, neuronal nuclear antigen. Color image is available online at www.liebertpub.com/neu

Effect of cannulation on silver staining

To determine whether cannulation produces axonal injury that may be masking the potentially beneficial effects of microglial depletion, we next determined the level of silver staining in CD11b-TK$^{-/-}$ sham mice alone ($n=5$; Fig. 14A,C), CD11b-TK$^{-/-}$ sham mice receiving i.c.v. saline by osmotic pump ($n=5$; Fig. 14B,D), and CD11b-TK$^{+/-}$ sham mice receiving intermediate-dose valganciclovir by osmotic pump ($n=5$; Fig. 14E,G). No difference was observed between groups (one-way ANOVA, $p=0.7006$; Fig. 14F). This indicates that contralateral cerebroventricular cannulation did not produce significant axonal injury in the ipsilateral CC ROI.

Astrocyte response in valganciclovir-treated mice

To confirm that only microglial numbers are being altered in this model, we analyzed the numbers of GFAP-positive astrocytes in regions of microglial depletion. We did not observe any change in the numbers of GFAP-positive astrocytes in the CC and EC of mice treated with 1 mg/mL of valganciclovir or 0.9% NaCl for 14 days (two-way ANOVA, genotype $p=0.6028$, treatment $p=0.9339$, genotype × treatment $p=0.7852$; Fig. 15A–C). Similarly, there were no apparent changes in astrocytes resulting from valganciclovir treatment within gray matter areas.

Inflammatory response in valganciclovir-treated mice

To determine how the inflammatory response was affected by microglial depletion in the setting of TBI, RNA was purified from injured and uninjured mice acutely treated (14 days total) with 10 mg/mL of valganciclovir and the amount of TNF-α, IL-1β, IL-6, iNOS, and CCL2 messenger RNA (mRNA) was determined by qPCR (Fig. 16A–E). Injury alone appeared to result in, at most, modest (<5-fold) increases in expression of these genes (rcTBI vs. sham CD11b$^{-/-}$ mice; Fig. 16A–E). Surprisingly, treatment of CD11b$^{+/-}$ mice with valganciclovir produced substantially greater changes in inflammatory gene expression in both injured and

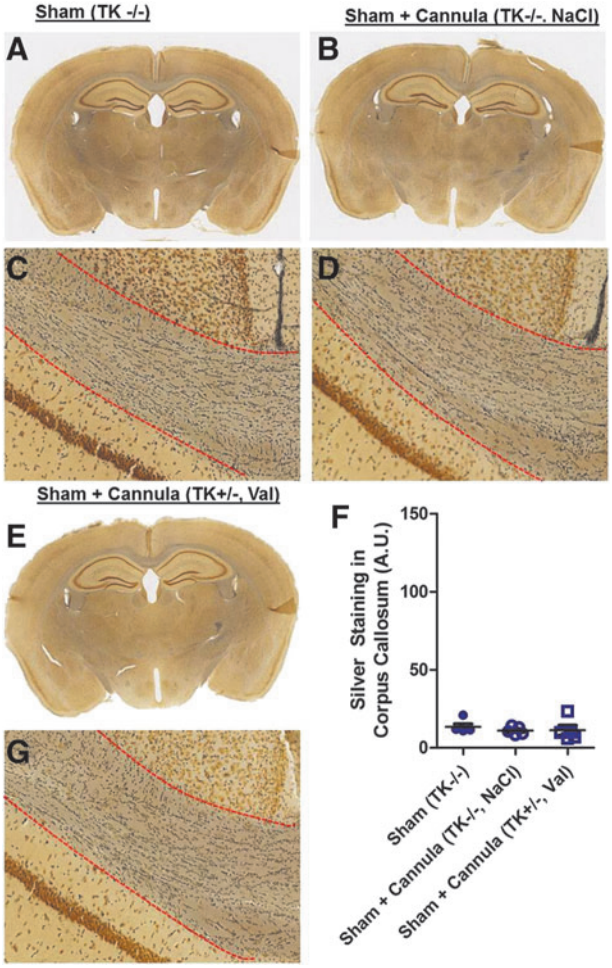

FIG. 14. Right-sided cerebroventricular cannulation does not contribute to silver staining in the left corpus callosum region of interest assessed for axonal injury. Silver staining was performed in sections from CD11b-TK$^{-/-}$ mice that underwent the sham procedure alone (**A** and **C**) or the sham procedure plus cannulation and treatment with saline (NaCl; **B** and **D**). Silver staining was also performed in sections from CD11b-TK$^{+/-}$ mice that underwent the sham procedure plus cannulation and treatment with 10 mg/mL of valganciclovir (**E** and **G**). All mice were sacrificed 7 days post–sham injury. (**F**) No difference in silver staining was observed between groups. A.U., arbitrary units; TK, thymidine kinase. Color image is available online at www.liebertpub.com/neu

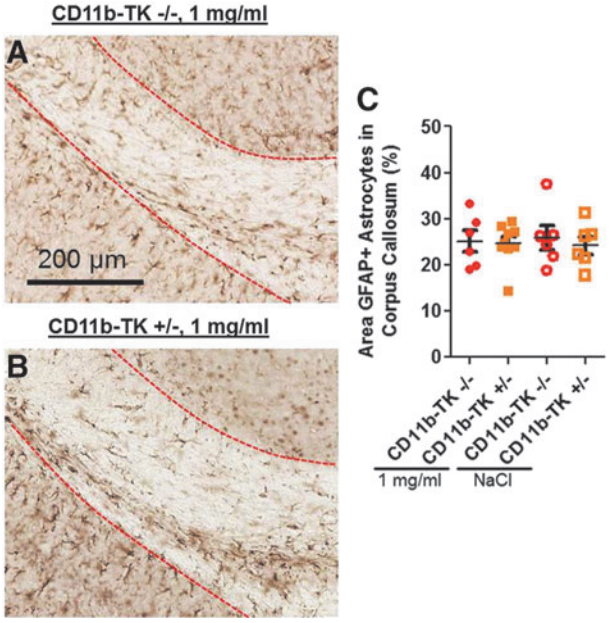

FIG. 15. Astrocytes 7 days after repetitive closed-skull traumatic brain injury in mice treated with 1 mg/mL of valganciclovir or NaCl. GFAP staining in treated CD11b-TK$^{-/-}$ (**A**) and CD11b-TK$^{+/-}$ (**B**) mice. (**C**) No differences in GFAP optical density was observed between groups. GFAP, glial fibrillary acidic protein; TK, thymidine kinase. Color image is available online at www.liebertpub.com/neu

uninjured mice. Qualitatively, only TNF-α appears to be increased to a greater extent in CD11b-TK$^{+/-}$ injured versus uninjured mice (Fig. 16E). Thus, whereas valganciclovir treatment of CD11b-TK mice reduces microglial cells, it may also drastically alter the inflammatory environment in this model.

Discussion

In summary, we found that a reduction of the microglial population within the CC and EC by 35–56% neither increases nor decreases the extent of silver staining abnormalities. The most likely interpretation is that while microglia migrate to, and proliferate around, areas of axonal injury, overall they remain neutral in regard to the early processes of axon degeneration. We also provide further evidence that the CD11b-TK mouse line is a powerful tool for manipulating the microglial and macrophage response, but show that the dose of valganciclovir must be carefully determined to prevent unintended, nonspecific toxicity and altered inflammatory gene expression in the central nervous system.

These studies are important because, to our knowledge, there are no previous reports directly addressing the relationship between microglia and axon injury after *in vivo* mild repetitive TBI. Researchers have used minocycline to reduce microglial activation, where it was reported to reduce brain lesion volume, caspase 1 activation, and cerebral edema after closed-skull TBI in mouse.[40–43] However, only one of these studies measured axonal injury (by APP IHC), and similar to results reported here, no difference was observed between minocycline- and vehicle-treated mice, despite a 59% reduction in microglial activation.[43] In another study in rats, administration of ''anti-inflammatory'' doses of ibuprofen for 4 months post–moderate fluid percussion TBI worsened performance on Morris water maze, a test of spatial learning and memory, compared to vehicle-treated rats.[44] The effect of treatment on microgliosis and axonal injury were not assessed. In the present study, we similarly reduced the number of microglia present in WM tracts and assayed axonal injury using multiple injury markers and electron microscopy. This study is limited, however, in that we cannot rule out the possibility of functional consequences to the depletion of microglia, independent of histological abnormalities.[45] In addition, this study is also limited in that it is possible that the maximum reduction of the microglial population by 56% was not enough to produce an effect on WM integrity. The remaining microglia may be able to compensate for the loss by ramping up production of secreted factors. Indeed, qPCR analysis revealed considerably more TNF-α, IL1-β, IL-6, iNOS, and CCL2 mRNA after valganciclovir treatment. These factors may directly impair axons or modulate the inflammatory response in a complex fashion.[46–48] Given this increase, it is

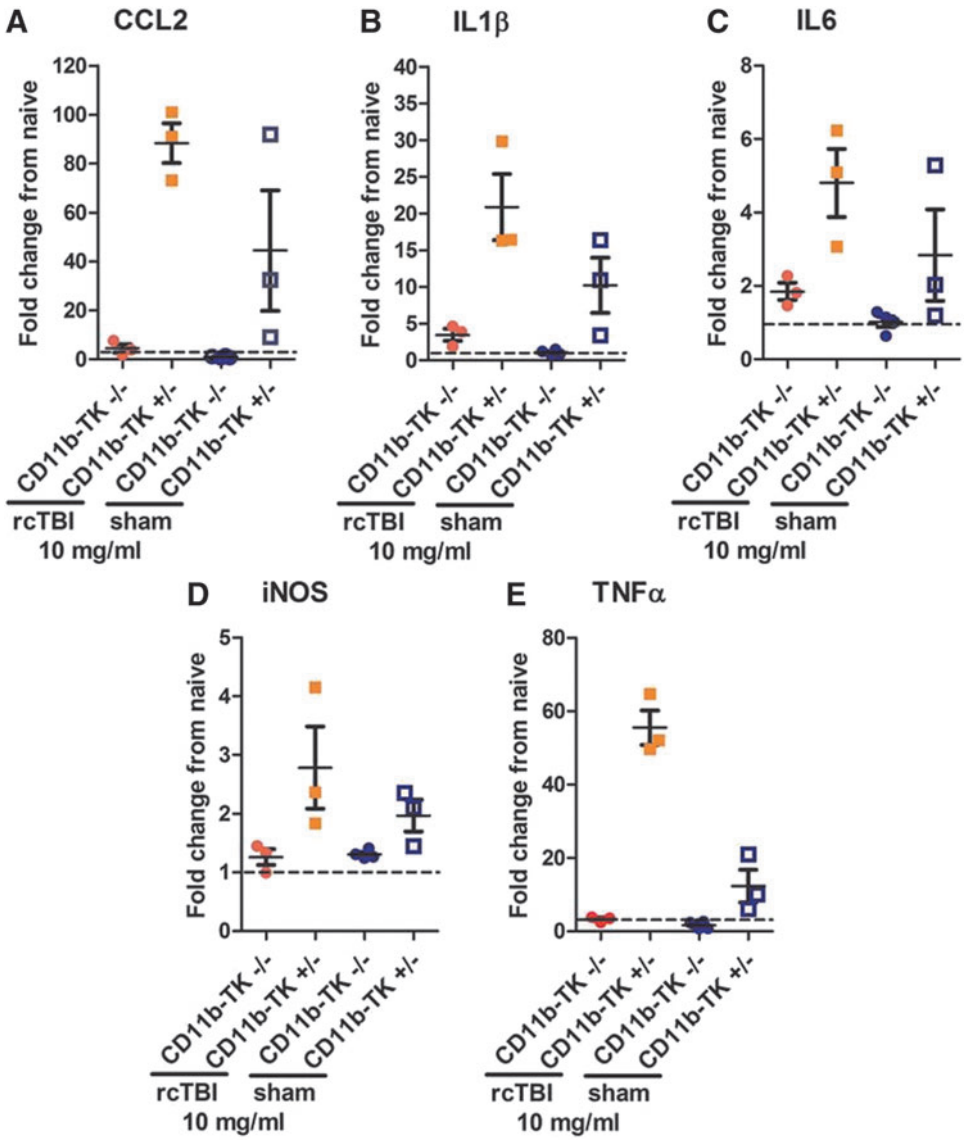

FIG. 16. qPCR measurement of inflammatory gene expression. Relative expression of (A) *Ccl2*, (B) *Il1β*, (C) *Il6*, (D) *iNOS*, and (E) *Tnfα* in each mouse was normalized first to the geometric mean of 3 reference genes (*Hprt, Pgk1, Gapdh*) and then to arithmetic mean of the uninjured, naïve mice (n = 4; dashed line). CCL2, chemokine (C-C motif) ligand 2; IL, interleukin; iNOS, inducible nitric oxide synthetase; TNF-α, tumor necrosis factor alpha; rcTBI, repetitive closed-skull traumatic brain injury; TK, thymidine kinase. Color image is available online at www.liebertpub.com/neu

remarkable that more-severe silver staining abnormalities were not detected. This could indicate that axons are resilient to many aspects of the inflammatory response. An important line of future investigation will involve elucidating the full time course of the changes in cytokine expression in response to injury and valganciclovir administration. Whether microglia and macrophages were directly responsible for the increases in secreted cytokine mRNA or whether the reduction in microglia induced expression by other cell types was not examined. Another alternative explanation for our results is that there could be both beneficial and harmful subtypes of microglia that are approximately evenly reduced by the experimental manipulations resulting in a net neutral effect on WM.[49] A final alternative explanation could be that any beneficial effects of microglial reduction were offset by the up-regulation of inflammatory gene expression in response to the valganciclovir treatment.

This study was also limited in that it did not assess the specific contribution of the resident microglial population versus peripheral macrophages to injury. In this injury model, however, we have not observed IgG accumulation or a large population of $CD45^{+hi}$, $CD11b^{+}$ cells (unpublished observations) that would be indicative of infiltration of peripheral macrophages. Thus, while peripheral macrophages may be present in rcTBI brains, most Iba-1 positive cells are likely resident microglia.

Although these data indicate that microglial cells are likely neutral overall in regard to axon injury after repetitive concussion in the acute and subacute phase, it remains mysterious why microglial cells migrate to the CC and EC and remain activated over the long term. Activated microglia and macrophage have been observed in the CC and other brain regions in human TBI patients several months or years after injury, indicating this is not a

mouse-specific phenomenon.[10,16,23] Because these are phagocytic cells, it may be that ongoing axon degeneration results in debris that stimulates the microglial response. Microglial clearance of this debris may be neither beneficial nor harmful in the relatively short time scale assessed in these experiments, but could play an important role in long-term chronic sequelae of injury, including axonal sprouting and regeneration not assessed here.[50] Indeed, microglia are important sources of brain-derived neurotrophic factor and other neurotrophins that stimulate axonal sprouting and may be central to recovery from injury.[51,52] Future work may help to address these questions and provide deeper insight into the biological function of microglia after injury. Other studies may also address the effect of microglial reduction in more-severe brain injury, where the role of microglial cells may be distinct.[53,54]

A technical note regarding the toxicity of valganciclovir in CD11b-TK mice warrants discussion. It was surprising that valganciclovir administration at intermediate and high doses produced such widespread tissue loss in CD11b-TK mice. Work from Grathwohl and colleagues has previously reported that administration of 50 mg/mL of valganciclovir can produce microhemorrhages after 1 month of treatment.[36] Their group was using an independently derived line of CD11b-TK mice. Mice used in our experiments were generated in the lab of Jean-Pierre Julien, and the thymidine kinase gene contains a mutation resulting in increased sensitivity to drug treatment. This increased sensitivity could explain why 10 mg/mL was sufficient to produce toxicity after 28 days and 50 mg/mL increased mortality by 50% after 14 days of treatment in our experiments. The underlying cause of this toxicity is unknown; the profoundly up-regulated cytokine mRNA levels detected by qPCR may indicate either a cause or an effect of the toxicity.

Altogether, the finding that microglia appear to be neutral in regard to injury is an important consideration for the design of future therapeutics. This could indicate that drugs specifically targeting axonal injury may be more useful after concussive-type injuries than those targeting microglial cells. Alternatively, methods to more completely prevent the activation and/or proliferation of microglial cells without toxicity should be sought for further studies.

Acknowledgments

The authors thank Dr. Jean-Pierre Julien (CHUL Research Center, Québec City, Québec, Canada) for generously sharing CD11b-TK mice and Thomas Esparza, Hien Tran, Krikor Dikranian, Marilyn Levy, and Yoshi Shitaka for their advice and help with methods development. The authors also thank the National Institutes of Health (NIH F31-NS076047 [to R.E.B.] and NIH R01-NS065069 [to D.L.B.]), and the Alafi Neuroimaging Core and Washington University.

Author Disclosure Statement

No competing financial interests exist.

References

1. Corsellis, J.A., Bruton, C.J., and Freeman-Browne, D. (1973). The aftermath of boxing. Psychol. Med. 3, 270–303.
2. Mortimer, J.A. (1985). Epidemiology of post-traumatic encephalopathy in boxers. Minn. Med. 68, 299–300.
3. Roberts, G.W., Allsop, D., and Bruton, C. (1990). The occult aftermath of boxing. J. Neurol. Neurosurg. Psychiatry 53, 373–378.
4. Geddes, J.F., Vowles, G.H., Nicoll, J.A., and Revesz, T. (1999). Neuronal cytoskeletal changes are an early consequence of repetitive head injury. Acta Neuropathol. 98, 171–178.
5. Guo Z, Cupples LA, Kurz A, Auerbach SH, Volicer L, Chui H, Green RC, Sadovnick AD, Duara R, DeCarli C, Johnson K, Go RC, Growdon JH, Haines JL, Kukull WA, and Farrer L.A. (2000). Head injury and the risk of AD in the MIRAGE study. Neurology 54, 1316–1323.
6. Guskiewicz, K.M., McCrea, M., Marshall, S.W., Cantu, R.C., Randolph, C., Barr, W., Onate, J.A., and Kelly, J.P. (2003). Cumulative effects associated with recurrent concussion in collegiate football players: the NCAA Concussion Study. JAMA 290, 2549–2555.
7. McCrea, M., Guskiewicz, K.M., Marshall, S.W., Barr, W., Randolph, C., Cantu, R.C., Onate, J.A., Yang J., and Kelly, J.P. (2003). Acute effects and recovery time following concussion in collegiate football players: the NCAA Concussion Study. JAMA 290, 2556–2563.
8. Guskiewicz, K.M., Marshall, S.W., Bailes, J., McCrea, M., Cantu, R.C., Randolph, C., and Jordan, B.D. (2005). Association between recurrent concussion and late-life cognitive impairment in retired professional football players. Neurosurgery 57, 719–726; discussion, 719–726.
9. McKee, A.C., Cantu, R.C., Nowinski, C.J., Hedley-Whyte, E.T., Gavett, B.E., Budson, A.E., Santini, V.E., Lee, H.S., Kubilus, C.A., and Stern R.A. (2009). Chronic traumatic encephalopathy in athletes: progressive tauopathy after repetitive head injury. J. Neuropathol. Exp. Neurol. 68, 709–735.
10. Oppenheimer, D.R. (1968). Microscopic lesions in the brain following head injury. J. Neurol. Neurosurg. Psychiatry 31, 299–306.
11. Adams, J.H., Graham, D.I., Murray, L.S., and Scott, G. (1982). Diffuse axonal injury due to nonmissile head injury in humans: an analysis of 45 cases. Ann. Neurol. 12, 557–563.
12. Blumbergs, P.C., Jones, N.R., and North, J.B. (1989). Diffuse axonal injury in head trauma. J. Neurol. Neurosurg. Psychiatry 52, 838–841.
13. Gultekin, S.H., and Smith, T.W. (1994). Diffuse axonal injury in craniocerebral trauma. A comparative histologic and immunohistochemical study. Arch. Pathol. Lab. Med. 118, 168–171.
14. Chen. X.H., Johnson. V.E., Uryu. K., Trojanowski. J.Q., and Smith, D.H. (2009). A lack of amyloid beta plaques despite persistent accumulation of amyloid beta in axons of long-term survivors of traumatic brain injury. Brain Pathol. 19, 214–223.
15. Goldstein, L.E., Fisher, A.M., Tagge, C.A., Zhang, X.L., Velisek, L., Sullivan, J.A., Upreti, C., Kracht, J.M., Ericsson, M., Wojnarowicz, M.W., Goletiani, C.J., Maglakelidze, G.M., Casey, N., Moncaster, J.A., Minaeva, O., Moir, R.D., Nowinski, C.J., Stern, R.A., Cantu, R.C., Geiling, J., Blusztajn, J.K., Wolozin, B.L., Ikezu, T., Stein, T.D., Budson, A.E., Kowall, N.W., Chargin, D., Sharon, A., Saman, S., Hall, G.F., Moss, W.C., Cleveland, R.O., Tanzi, R.E., Stanton, P.K., and McKee, A.C. (2012). Chronic traumatic encephalopathy in blast-exposed military veterans and a blast neurotrauma mouse model. Sci. Transl. Med. 4, 134ra160.
16. Johnson, V.E., Stewart, J.E., Begbie, F.D., Trojanowski, J.Q., Smith, D.H., and Stewart, W. (2013). Inflammation and white matter degeneration persist for years after a single traumatic brain injury. Brain 136, 28–42.
17. McKee, A.C., Stein, T.D., Nowinski, C.J., Stern, R.A., Daneshvar, D.H., Alvarez, V.E., Lee, H.S., Hall, G., Wojtowicz, S.M., Baugh, C.M., Riley, D.O., Kubilus, C.A., Cormier, K.A., Jacobs, M.A., Martin, B.R., Abraham, C.R., Ikezu, T., Reichard, R.R., Wolozin, B.L., Budson, A.E., Goldstein, L.E., Kowall, N.W., and Cantu, R.C. (2013). The spectrum of disease in chronic traumatic encephalopathy. Brain 136, 43–64.
18. Chappell, M.H., Ulug, A.M., Zhang, L., Heitger, M.H., Jordan, B.D., Zimmerman, R.D., and Watts, R. (2006). Distribution of microstructural damage in the brains of professional boxers: a diffusion MRI study. J. Magn. Reson. Imaging 24, 537–542.
19. Zhang, L., Heier, L.A., Zimmerman, R.D., Jordan, B., and Ulug, A.M. (2006). Diffusion anisotropy changes in the brains of professional boxers. AJNR Am. J. Neuroradiol. 27, 2000–2004.
20. Zhang, K., Johnson, B., Pennell, D., Ray, W., Sebastianelli, W., and Slobounov, S. (2010). Are functional deficits in concussed individuals consistent with white matter structural alterations: combined FMRI & DTI study. Exp. Brain Res. 204, 57–70.
21. Cubon, V.A., Putukian, M., Boyer, C., and Dettwiler, A. (2011). A diffusion tensor imaging study on the white matter skeleton in individuals with sports-related concussion. J. Neurotrauma 28, 189–201.
22. Henry, L.C., Tremblay, J., Tremblay, S., Lee, A., Brun, C., Lepore, N., Theoret, H., Ellemberg, D., and Lassonde, M. (2011). Acute and chronic changes in diffusivity measures after sports concussion. J. Neurotrauma 28, 2049–2059.

23. Ramlackhansingh, A.F., Brooks, D.J., Greenwood, R.J., Bose, S.K., Turkheimer, F.E., Kinnunen, K.M., Gentleman, S., Heckemann, R.A., Gunanayagam, K., Gelosa, G., and Sharp, D.J. (2011). Inflammation after trauma: microglial activation and traumatic brain injury. Ann. Neurol. 70, 374–383.
24. Bazarian, J.J., Zhu, T., Blyth, B., Borrino, A., and Zhong, J. (2012). Subject-specific changes in brain white matter on diffusion tensor imaging after sports-related concussion. Magn. Reson. Imaging 30, 171–180.
25. Laurer, H.L., Bareyre, F.M., Lee, V.M., Trojanowski, J.Q., Longhi, L., Hoover, R., Saatman, K.E., Raghupathi, R., Hoshino, S., Grady, M.S., and McIntosh, T.K. (2001). Mild head injury increasing the brain's vulnerability to a second concussive impact. J. Neurosurg. 95, 859–870.
26. Uryu, K., Laurer, H., McIntosh, T., Pratico, D., Martinez, D., Leight, S., Lee, V.M., and Trojanowski, J.Q. (2002). Repetitive mild brain trauma accelerates Abeta deposition, lipid peroxidation, and cognitive impairment in a transgenic mouse model of Alzheimer amyloidosis. J. Neurosci. 22, 446–454.
27. Creeley, C.E., Wozniak, D.F., Bayly, P.V., Olney, J.W., and Lewis, L.M. (2004). Multiple episodes of mild traumatic brain injury result in impaired cognitive performance in mice. Acad Emerg. Med. 11, 809–819.
28. Creed, J.A., DiLeonardi, A.M., Fox, D.P., Tessler, A.R., and Raghupathi, R. (2011). Concussive brain trauma in the mouse results in acute cognitive deficits and sustained impairment of axonal function. J. Neurotrauma 28, 547–563.
29. Shitaka, Y., Tran, H.T., Bennett, R.E., Sanchez, L., Levy, M.A., Dikranian, K., and Brody, D.L. (2011). Repetitive closed-skull traumatic brain injury in mice causes persistent multifocal axonal injury and microglial reactivity. J. Neuropathol. Exp. Neurol. 70, 551–567.
30. Mouzon, B., Chaytow, H., Crynen, G., Bachmeier, C., Stewart, J., Mullan, M., Stewart, W., and Crawford, F. (2012). Repetitive mild traumatic brain injury in a mouse model produces learning and memory deficits accompanied by histological changes. J. Neurotrauma 29, 2761–2773.
31. Gowing, G., Vallieres, L., and Julien, J.P. (2006). Mouse model for ablation of proliferating microglia in acute CNS injuries. Glia 53, 331–337.
32. Heppner, F.L., Greter, M., Marino, D., Falsig, J., Raivich, G., Hovelmeyer, N., Waisman, A., Rulicke, T., Prinz, M., Priller, J., Becher, B., and Aguzzi, A. (2005). Experimental autoimmune encephalomyelitis repressed by microglial paralysis. Nat. Med. 11, 146–152.
33. DeVos, S.L., and Miller, T.M. (2013). Direct intraventricular delivery of drugs to the rodent central nervous system. J. Vis. Exp. e50326.
34. Simard, A.R., Soulet, D., Gowing, G., Julien, J.P., and Rivest, S. (2006). Bone marrow-derived microglia play a critical role in restricting senile plaque formation in Alzheimer's disease. Neuron 49, 489–502.
35. Varvel, N.H., Grathwohl, S.A., Baumann, F., Liebig, C., Bosch, A., Brawek, B., Thal, D.R., Charo, I.F., Heppner, F.L., Aguzzi, A., Garaschuk, O., Ransohoff, R.M., and Jucker, M. (2012). Microglial repopulation model reveals a robust homeostatic process for replacing CNS myeloid cells. Proc. Natl. Acad. Sci. U. S. A. 109, 18150–18155.
36. Grathwohl, S.A., Kalin, R.E., Bolmont, T., Prokop, S., Winkelmann, G., Kaeser, S.A., Odenthal, J., Radde, R., Eldh, T., Gandy, S., Aguzzi, A., Staufenbiel, M., Mathews, P.M., Wolburg, H., Heppner, F.L., and Jucker, M. (2009). Formation and maintenance of Alzheimer's disease beta-amyloid plaques in the absence of microglia. Nat. Neurosci. 12, 1361–1363.
37. Gentleman, S.M., Nash, M.J., Sweeting, C.J., Graham, D.I., and Roberts, G.W. (1993). Beta-amyloid precursor protein (beta APP) as a marker for axonal injury after head injury. Neurosci. Lett. 160, 139–144.
38. Sherriff, F.E., Bridges, L.R., and Sivaloganathan, S. (1994). Early detection of axonal injury after human head trauma using immunocytochemistry for beta-amyloid precursor protein. Acta Neuropathol. 87, 55–62.
39. Stone, J.R., Singleton, R.H., and Povlishock, J.T. (2001). Intra-axonal neurofilament compaction does not evoke local axonal swelling in all traumatically injured axons. Exp. Neurol. 172, 320–331.
40. Sanchez Mejia, R.O., Ona, V.O., Li, M., and Friedlander, R.M. (2001). Minocycline reduces traumatic brain injury-mediated caspase-1 activation, tissue damage, and neurological dysfunction. Neurosurgery 48, 1393–1399; discussion, 1399–1401.
41. Bye, N., Habgood, M.D., Callaway, J.K., Malakooti, N., Potter, A., Kossmann, T., and Morganti-Kossmann, M.C. (2007). Transient neuroprotection by minocycline following traumatic brain injury is associated with attenuated microglial activation but no changes in cell apoptosis or neutrophil infiltration. Exp. Neurol. 204, 220–233.
42. Homsi, S., Federico, F., Croci, N., Palmier, B., Plotkine, M., Marchand-Leroux, C., and Jafarian-Tehrani, M. (2009). Minocycline effects on cerebral edema: relations with inflammatory and oxidative stress markers following traumatic brain injury in mice. Brain Res. 1291, 122–132.
43. Homsi, S., Piaggio, T., Croci, N., Noble, F., Plotkine, M., Marchand-Leroux, C., and Jafarian-Tehrani, M. (2010). Blockade of acute microglial activation by minocycline promotes neuroprotection and reduces locomotor hyperactivity after closed head injury in mice: a twelve-week follow-up study. J. Neurotrauma 27, 911–921.
44. Browne, K.D., Iwata, A., Putt, M.E., and Smith, D.H. (2006). Chronic ibuprofen administration worsens cognitive outcome following traumatic brain injury in rats. Exp. Neurol. 201, 301–307.
45. Reeves, T.M., Phillips, L.L., and Povlishock, J.T. (2005). Myelinated and unmyelinated axons of the corpus callosum differ in vulnerability and functional recovery following traumatic brain injury. Exp. Neurol. 196, 126–137.
46. Ashki, N., Hayes, K.C., and Shi, R. (2006). Nitric oxide reversibly impairs axonal conduction in Guinea pig spinal cord. J. Neurotrauma 23, 1779–1793.
47. Davies, A.L., Hayes, K.C., and Shi, R. (2006). Recombinant human TNFalpha induces concentration-dependent and reversible alterations in the electrophysiological properties of axons in mammalian spinal cord. J. Neurotrauma 23, 1261–1273.
48. Morganti-Kossmann, M.C., Satgunaseelan, L., Bye, N., and Kossmann, T. (2007). Modulation of immune response by head injury. Injury 38, 1392–1400.
49. Kigerl, K.A., Gensel, J.C., Ankeny, D.P., Alexander, J.K.,, Donnelly, D.J., and Popovich, P.G. (2009). Identification of two distinct macrophage subsets with divergent effects causing either neurotoxicity or regeneration in the injured mouse spinal cord. J. Neurosci. 29, 13435–13444.
50. Hosmane, S., Tegenge, M.A., Rajbhandari, L., Uapinyoying, P., Kumar, N.G., Thakor, N., and Venkatesan, A. (2012). Toll/interleukin-1 receptor domain-containing adapter inducing interferon-beta mediates microglial phagocytosis of degenerating axons. J. Neurosci. 32, 7745–7757.
51. Batchelor, P.E., Porritt, M.J., Martinello, P., Parish, C.L., Liberatore, G.T., Donnan, G.A., and Howells, D.W. (2002). Macrophages and microglia produce local trophic gradients that stimulate axonal sprouting toward but not beyond the wound edge. Mol. Cell. Neurosci. 21, 436–453.
52. Venkatesan, C., Chrzaszcz, M., Choi, N., and Wainwright, M.S. (2010). Chronic upregulation of activated microglia immunoreactive for galectin-3/Mac-2 and nerve growth factor following diffuse axonal injury. J. Neuroinflammation 7, 32.
53. Jiang, Y., and Brody, D.L. (2012). Administration of COG1410 reduces axonal amyloid precursor protein immunoreactivity and microglial activation after controlled cortical impact in mice. J. Neurotrauma 29, 2332–2341.
54. Loane, D.J., Kumar, A., Stoica, B.A., Cabatbat, R., and Faden, A.I. (2014). Progressive neurodegeneration after experimental brain trauma: association with chronic microglial activation. J. Neuropathol. Exp. Neurol. 73, 14–29.

Address correspondence to:
David L. Brody, MD, PhD
Department of Neurology
Washington University
660 South Euclid Avenue
Campus Box 8111
St. Louis, MO 63110

E-mail: brodyd@neuro.wustl.edu